

1 **Introducing standardized field methods for fracture-focused surface**
2 **processes research**

3 Martha Cary Eppes¹, Alex Rinehart², Jennifer Aldred³, Samantha Berberich¹, Maxwell P. Dahlquist⁴, Sarah
4 G. Evans⁵, Russell Keanini⁶, Stephen E. Laubach⁷, Faye Moser¹, Mehdi Morovati⁶, Steven Porson¹, Monica
5 Rasmussen¹, Uri Shaanan⁸

6 ¹ Department of Geography & Earth Sciences, University of North Carolina at Charlotte, Charlotte, NC 28223, USA

7 ² Department of Earth and Environmental Sciences, New Mexico Institute of Mining and Technology, Socorro, NM, 87801, USA

8 ³ New Mexico Highlands University, Las Vegas, NM, USA

9 ⁴ Department of Geology, University of the South, Sewanee, TN 37383, USA

10 ⁵ Department of Geological and Environmental Sciences, Appalachian State University, Boone, NC, 28608, USA

11 ⁶ Department of Mechanical Engineering and Engineering Science, University of North Carolina at Charlotte, Charlotte, NC
12 28223, USA

13 ⁷ Jackson School of Geosciences, The University of Texas at Austin, Austin, TX 78714

14 ⁸ Geological Survey of Israel, Jerusalem 9692100, Israel

15 *Correspondence to:* meppes@charlotte.edu

16

17 **Abstract.** Rock fractures are a key contributor to a broad array of Earth surface processes due to their direct control on rock
18 strength as well as rock porosity and permeability. However, to date, there has been no standardization for the quantification of
19 rock fractures in surface processes research. In this work, the case is made for standardization within fracture-focused research,
20 and prior work is reviewed to identify various key datasets and methodologies. Then, a suite of standardized methods is presented
21 as a starting ‘baseline’ for fracture-based research in surface processes studies. These methods have been shown in preexisting
22 work from structural geology, geotechnical engineering, and surface processes disciplines to comprise best practices for the
23 characterization for fractures in clasts and outcrops. This practical, accessible, and detailed guide can be readily employed across
24 all fracture-focused weathering and geomorphology applications. The wide adoption of a baseline of data collected using the same
25 methods will enable comparison and compilation of datasets among studies globally and will ultimately lead to a better
26 understanding of the links and feedbacks between rock fracture and landscape evolution.

27
28 **Short Summary.** All rocks have fractures (cracks) that can influence virtually every process acting on Earth's surface where
29 humans live. Yet, scientists have not standardized their methods for collecting fracture data. Here we draw on past work across
30 geo-disciplines and propose a list of baseline data for fracture-focused surface processes research. We detail its rationale and the
31 methods for collecting it. We hope its wide adoption will improve future methods and knowledge of rock fracture overall.

32 **1 Introduction**

33 Rock fracture in surface and near-surface environments plays a key role in virtually all Earth surface processes. Fractures comprise
34 faults and opening-mode fractures; both coming in a wide range of sizes. The focus here, however, is on opening-mode fractures.
35 The propagation of opening-mode fractures universally occurs at or near the surface of Earth (e.g., within ~500 m - Moon et al.,
36 2020), on other terrestrial bodies (Molaro et al., 2020), and at depth in the crust (e.g., Laubach et al., 2019). It epitomizes mechanical
37 weathering and the development of ‘critical zone architecture’, i.e., the evolving porosity, permeability, and strength of near-
38 surface rock (e.g., Riebe et al., 2021). For clarity and consistency herein, the use of the term fracture is limited to refer to any *open*,
39 high-length-to-aperture-ratio discontinuity in rock, regardless of its origin, scale, or location (e.g. within a clast, or within shallow
40 or deep bedrock), acknowledging that veins (partly to completely mineral filled fractures) or dikes (filled with secondary minerals)
41 are also termed ‘fractures’ in many contexts. The term ‘crack’ is avoided because the wide-ranging semantics of that term can
42 cause confusion when employed in interdisciplinary work across rock mechanics, structural geology, and geomorphology.

43
44 Fracture characteristics (e.g., size, number, connectivity, orientation) exert enormous influence on both rock mechanical properties
45 (e.g., Ayatollahi and Akbaridoost, 2014) and rock hydrological properties (e.g., Leone et al., 2020; Snowdon et al., 2021). Fractures
46 therefore influence a wide array of natural and anthropogenic landscape features and processes including channel incision (e.g.,
47 Shobe et al., 2017), sediment size and production (Sousa, 2010; Sklar et al., 2017), hillslope erosion (e.g., DiBiase et al., 2018;
48 Neely et al., 2019), built environment degradation (e.g., Hatir, 2020), landslide and rockfall hazards (e.g., Collins and Stock, 2016),
49 groundwater and surface water processes (e.g., Maffucci et al., 2015; Wohl, 2008), and vegetation distribution (e.g., Aich and
50 Gross, 2008). Additionally, the resultant physical properties of fracture-produced sediment (i.e., clast size distribution, mass,
51 porosity, etc.) control both hillslope and stream processes (e.g., Chilton and Spotila, 2020; Glade et al., 2019).

52

53 With fractures clearly central to so many surface processes, as well as to non-academic concerns such as hazard and infrastructure
54 degradation, it is crucial to understand the factors that control surface and near-surface rock fracture attributes, and rock fracturing
55 rates and processes. To fully do so requires a large body of data quantifying fracture-related characteristics and phenomena in a
56 variety of subaerial environments; however, to date, no standard field methods have been widely adopted to quantify fractures in
57 the modern surface processes realm. Consequently, data collected across studies cannot be readily compared or coalesced. The
58 purpose of this paper is to define an initial set of such standards with the anticipation that the methods will evolve as new
59 understanding, needs and applications arise. We develop these proposed standards by combining prior fracture methodologies from
60 other geoscience disciplines with those that have been developed, tested and refined through more than 20 years of field-based
61 fracture observations for surface processes-related research (e.g., Aldred et al., 2015; Eppes and Griffing, 2010; Eppes et al., 2018;
62 Eppes et al., 2010; Mcfadden et al., 2005; Moser, 2017; Shobe et al., 2017; Weiserbs, 2017).

63
64 Building on past work, this paper defines the benefits of establishing a standard procedure for fracture-focused surface processes
65 field research, describing how presented methods outperform other approaches. We then provide a short review of motivating
66 existing approaches derived primarily from engineering and structural geology disciplines. Finally, we describe a set of methods
67 that is proposed as a starting point for surface processes researchers so that a larger community of teams can begin to cross-pollinate
68 their observations. When no other standard practice is evident in existing literature, we have suggested rules of thumb that are
69 based on our experience during fieldwork for past published works (e.g. Eppes and McFadden, 2010; Aldred et al., 2016; Ortega
70 et al., 2006). We explicitly note when such practices are presented, and our rationale thereof. The overall scope herein is limited
71 to in-person field observations on sub-aerially exposed rock, i.e., fractures that can be observed with the naked eye or basic hand
72 lens. Measurements of smaller fractures (e.g., those visible with microscopy) or of buried fractures (e.g., those visualized in
73 boreholes or with indirect geophysical methods) are not directly described here. We also note that methods for fracture detection
74 using automated analyses of remote data such as LiDAR, drone photography, structure-from-motion, or 3D modeling are not
75 described herein, but provide motivation for this work (Sect. 1.2).

76
77 In sum, the overall aim of this paper is to build: 1) a motivation for standardization based on existing published work across
78 disciplines 2) a set of guiding principles applicable to all surface processes research involving rock fractures; 3) a list of fracture
79 and rock data measurements that constitute “basic” field-based metrics; and 4) practical methods that comprise best practices for
80 collection of these data. Unless otherwise specified, all methods may be applied to loose clasts or to outcrops. Also provided are
81 some suggestions for data analyses and a demonstration of a real case example of how the proposed methods lead to reproducible
82 results across users. By providing this compendium of fracture-focused field methods, the hope is to accelerate understanding of
83 how a most basic feature of all rock – its open fractures – contributes to the processes and evolution of Earth’s surface and critical
84 zone.

85 1.1 The value of a standardized approach

86 Particularly within the fields of geomorphology and weathering sciences, no common suite of data, methods, or terminology has
87 been defined or described that comprises an analysis of fractures. Although fracture characterization field methods exist in the
88 context of structural geology and aquifer and reservoir characterization (e.g., Watkins et al., 2015; Wu and Pollard, 1995; Zeeb et
89 al., 2013; Laubach et al., 2018), they diverge significantly in their approaches because they were largely developed for the specific

90 application of each unique study or field of study. Furthermore, the terminology and methodologies used to describe natural
91 fractures across this existing research tend to be applicable to what is typically envisioned as deep-seated processes including
92 tectonic loading and pore pressure elevation (e.g., Schultz, 2019). Numerous published works fail to provide clear criteria for
93 categorizing fractures, or even for choosing which fractures to measure. The choices, of course, depend on the objectives of the
94 study. This lack of consistency severely limits the ability of the geomorphic community to reproduce methods, or to combine,
95 compare, or interpret different fracture datasets.

96
97 The development of consistent methods undergirds most quantitative Earth sciences. For example, the fields of sedimentology and
98 soil science have clear, standardized methods to acquire what constitutes the “basic” data for their observations. Sedimentologists
99 have long shared common metrics and methods for quantifying grain size, sorting, rounding, and stratigraphic records (e.g.,
100 Krumbein, 1943). Similarly, soil scientists share common methods, metrics, and nomenclature for describing soil profiles and
101 horizons (e.g., Birkeland, 1999 Appendix A; Soil Survey Staff, 1999). The realization of the need for standard methods has also
102 remained constant in laboratory-based rock mechanics over the last several decades, driving the American Society for Testing and
103 Materials (ASTM) and International Society for Rock Mechanics (ISMR) to publish ongoing standards and methods papers (e.g.,
104 Ulusay and Hudson, 2007; Ulusay, 2015).

105
106 Standards like those mentioned above exist because workers have long recognized and reaped their benefits. Standardized methods
107 can frequently lead to major step-change innovations when data are combined. For example, standardized soil methods allowed
108 for 100 m scale mapping across the United States, enabling detailed human–landscape models that can aid in preserving vital soil
109 resources (Ramcharan et al., 2018). In the field of rock mechanics prior to the 1950s, theoretical developments of rock failure and
110 plasticity lagged other branches of geophysics and engineering. It is likely that progress was limited not only by technology but,
111 arguably more so, by lack of consistent methods. Methods for repeatable failure testing were then developed, largely in the groups
112 led by Knoppf, Griggs, and Turner in the United States and Australia (Wenk, 1979). This standardization culminated in the
113 landmark series of papers that comprised the observations driving 50 subsequent years of experimental rock mechanics (e.g., Borg
114 and Handin, 1966; Handin et al., 1963; Handin and Hager, 1957, 1958; Heard, 1963; Mogi, 1967, 1971; Turner et al., 1954).

115 116 **1.2 Existing fracture measurement approaches across disciplines**

117 For the specific case of fracture-focused research, outside of geomorphology applications, the need for standardized rule-based
118 methods has already been established. Within this prior body of research, engineering and structural geology applications have
119 dominated the development of various approaches.

120
121 Engineering geology and geotechnical engineering share common practices in mapping different standards of rock quality and
122 rock mass classification, of which fracture characterization is an important component. The rock quality designation (RQD) was
123 developed in the early 1960s to predict rock mass suitability for building, foundations, tunneling, and other geotechnical issues
124 (Deere, 1964 in Bell, 2007). Within that work, the primary concern is the integrity of the rock, which is governed by its
125 discontinuities, primarily fractures. By providing a standard approach to defining rock quality - albeit qualitative or semi-
126 quantitative - the development of a globally accepted basis of rock mass classification built from RQD and discontinuity surveys
127 has provided a common language for engineering geologists and geotechnical engineers to discuss site suitability and to design

128 critical infrastructure to the point that slope stability parameters, hydrologic suitability and intact strength can be broadly predicted
129 (Bell, 2007; Hencher, 2012; Hencher, 2015). Thus, such rock quality metrics may be appropriate for surface processes applications,
130 and they provide a rationale and basis for the use of the semi-quantitative methods presented herein.

131

132 The rock quality index consists of qualitative classifications from very poor (RQD 0 to 25%) to excellent (RQD 90 to 100%) based
133 on the linear fracture frequency in core or outcrop line surveys, laboratory velocity measurements, or the ratio of the deformability
134 of the rock mass to that of intact rock (Bell, 2007). Specifically for fractures, rock quality designations are derived only from counts
135 of the number of fractures per foot or core or outcrop. More quantitative estimates of outcrop rock mass quality – commonly used
136 to estimate slope stability quantities – involve measuring multiple lines on an outcrop with estimates of fracture aperture width,
137 hydrologic state (closed, cemented, partially open, open and flowing), fracture orientation, strength of intact rock estimated with a
138 rock hammer, degree of weathering, and fracture ‘roughness’ or relief along a line of a fixed length, commonly 20 m to 30 m (Bell,
139 2007). These surveys are then repeated periodically with a spacing of ~100 m, depending on the application (Bell, 2007). Similar
140 methods are used with core and image logging tools (Hencher, 2012; Hencher 2015). The fracture parameters are then used in a
141 variety of index models that predict the bulk strength, hydraulic conductivity, and stability of the rock mass. Thus, the extensiveness
142 of the list of measured rock- and fracture- characteristics in the geotechnical engineering literature reflects the variety of impacts
143 that they have both on each other and on the behavior of the rock mass. Here a similar comprehensive list is proposed, but more
144 with surface processes applications in mind, and thus applicable to a larger range of scale of fractures.

145

146 Measurements of the length and aperture of fractures that intersect a line (scanlines), similar to those used for engineering rock
147 quality applications, are widely used and effective in structural geology applications (Marrett et al., 2018; Hooker et al., 2009),
148 and may be valuable where exposures approximate a 1D sample. Selection bias can be avoided by randomly picking scanline
149 directions or by measuring multiple scanlines. To capture all fracture orientations geometric corrections are needed (e.g., Terzaghi,
150 1965; Wang et al., 2023). When fractures are oblique to scanlines, these corrections are generally more effective if scanlines are
151 long relative to fracture occurrence. Calculations of fracture number density and fracture intensity (Section 6.1) require corrections
152 for comparison with 2D data. Depending on the heterogeneity and anisotropy of host rocks, long 1D measures may complicate
153 comparison of fracture patterns to rock properties. Although they are well suited for capturing the most reproducible and unbiased
154 measure for fracture size, namely fracture aperture distributions (e.g., Marrett et al., 2018) as a 1D measure, without extra
155 measurement steps, scanlines are not well suited for characterizing representative 2D or 3D rock characteristics or for measuring
156 fracture lengths, heights, or connectivity, all important to surface processes. Thus, in the proposed methods herein, the focus is on
157 2D ‘windows’, and an expansion of fracture length measurements – like that proposed by Weiss (2008) – is also detailed so that
158 long fractures are not underrepresented (Section 5.4.1).

159

160 For 2D characterizations, Zeeb et al. (2013) sought to determine how different sampling approaches lead to censoring bias of
161 different fracture sizes from outcrop data by applying different sampling methods to artificially generated fracture networks that
162 had known parameters. Analysis of data collected using scanline, window, and circular estimator methods revealed that the window
163 approach resulted in the lowest uncertainty for most parameters and required the fewest measurements to provide representative
164 datasets. For areas with large outcrop exposures, circular scanlines combined with a window approach have proven effective
165 (Watkins et al., 2015). Scanlines are also helpful in characterizing simple fracture spatial arrangement attributes. Here, a ‘window’

166 approach is outlined that can be employed regardless of outcrop size or fracture number density, both of which could vary
167 considerably in any given surface process field area.

168
169 Another consideration that arises in both structural geology and the engineering applications is that the methods of fracture (and
170 rock) characterization must include accommodation for rock variations, and discipline-specific considerations for specific sites
171 (Hencher, 2012). In particular, the total area(s) of observation and numbers of fractures examined must always be normalized for
172 the specific rock and/or location within the ‘fracture stratigraphy’ of a study (e.g., Laubach et al., 2009). For example, it is common
173 for sandstone and shaly sandstone to both occur over short distances, and that their fracture abundance will vary by rock type (for
174 example, clay-poor sandstones tend to be more brittle and fracture prone). In this circumstance, the lithologic control on abundance
175 is identified first (this can be qualitative), then the abundance measures are normalized to area of the specific rock type. For
176 example, Hooker et al. (2013) employs a reverse procedure, whereby multivariate measures are used to isolate the rock type to
177 which normalization should be confined (if any). A further caution is that all fracture populations in the same rock may not reflect
178 the attributes of the host rock in the same way (all parts of the fracture population may not even be present in all rock types). This
179 variance may arise if fractures are not all the same age; because differences in loading paths, exposure histories, and rock properties
180 may vary. Engineering geology applications often map fracture populations in a similar way (Hencher, 2012; 2015) but without
181 the geologic context. Instead, zones are identified and cross-cutting relationships of fractures are commonly used to identify
182 primary vs. secondary planes of weakness. The methods presented herein include instructions for how to make these overall
183 judgements of necessary accommodations and normalizations.

184
185 Just as fracture characterization methods must be developed to accommodate variance between and across rock types, they must
186 also be developed so that they are reproducible across users. Above all, it has been established that reproducibility requires clear,
187 rule-based criteria for all decision-making (Forstner and Laubach, 2022). Forstner and Laubach (2022) and Ortega and Marrett
188 (2000) detail issues that arise, particularly from a lack of specificity with respect to identifying features to be measured. In another
189 case example (Andrews et al., 2019), study participants were asked to measure fractures with no particular instructions given for
190 how to collect the data other than where to collect it. The wide variance in resulting datasets collected by different users led to the
191 conclusion that, without common and clearly established measurement and selection criteria, fracture characterization is rife with
192 subjective bias that severely impacts interpretations of results. Then, based on post-data collection interviews and workshops,
193 Andrews et al. (2019) scrutinized the source of the variance and provided a list of suggested best-practices that would serve to best
194 eliminate the subjectivity of data collection that was leading to the bias. In engineering contexts, it is more common to handle such
195 possibility of bias by having fracture mapping during site investigations be performed by a single engineering geologist or by a
196 single, small team of trained engineers or geologists (Hencher, 2012). Ideally, either would be carefully reviewed by a senior
197 engineering geology professional. These fracture maps are incorporated into the site model, which is updated – preferably by the
198 same engineering geologist – during construction. In case studies, it is common for poor quality or inconsistent fracture mapping
199 to lead to incorrectly designed structures, which may fail (Hencher, 2012). Despite these often-dramatic failures, the site-specific
200 nature of fracture networks during rock mass characterization and the balance for a financially successful project may lead to poor
201 review and oversight practices while developing a site model (Hencher, 2012). Here, so that users from different groups may
202 consistently employ this field guide, clear, rules-based criteria are provided that may be used for all measurements described and
203 justify the criteria based on past work and experience.

204

205 Including that described above, incorporated in this work are suggested best practices from existing published methods research.
206 For example, field measurement ‘crack comparators’ are effective for measuring opening displacements particularly for sub-
207 millimeter widths (e.g., Ortega et al., 2006). Other measurements such as length and connectivity may have low reproducibility
208 (Andrews et al., 2019) owing to various observational and conceptual problems, including dependence on scale of observation
209 (e.g., Ortega and Marrett, 2000).

210

211 In addition to existing field based fracture research, remote sensing technologies such as lidar, drone photogrammetry, and structure
212 from motion, are becoming increasingly common to enable the production of fracture maps whose properties can then be quantified
213 and characterized digitally using freely available software packages such as FracPaQ (Healy et al., 2017). These technologies are
214 rapidly evolving and hold great promise for expanding the scope of fracture measurements overall (e.g. Betlem et al., 2022; Zeng
215 et al., 2023). To date, however, mapping fractures using these techniques holds limitations such as difficulty distinguishing between
216 fractures and edges, and are not readily accessible to all field scientists. We believe that it would be premature, and is also beyond
217 the scope of our goals, to try to distill those methods into best practices. Instead, we assert that the methods outlined herein represent
218 a consistent set of methods that could be employed for validation across all such remotely sensed data collection. Furthermore,
219 many of the field methods described herein, such as site and observation area selection, are required for any fracture mapping
220 effort regardless of technique. Thus, many of the methods we present can be applied to most studies using these rapidly evolving
221 remote sensing technologies and should aide in accelerating their development.

222

223 Finally, in all cases, the chosen standardized methods presented are optimized for collecting outcrop- and clast-fracture data
224 relevant to geomorphology and other surface process-based disciplines (e.g. critical zone sciences, building stone preservation,
225 hydrogeology). The methods described herein are germane to surface and near-surface (< 0.5 km) studies such as validating
226 geophysical measurements, testing factors that influence fracture formation, or documenting links between fracture characteristics
227 and topography or sediment production. Due to a lack of explicit knowledge suggesting otherwise, we present these methods based
228 on an assumption that fractures of all scales (um to km) contribute to all surface processes. Thus, these methods may differ from
229 those of studies with other goals, such as using outcrops as analogs for deep (km scale) subsurface fractures. Such studies aim to
230 distinguish mechanical and fracture stratigraphy, corroborate fracture patterns related to features (i.e., folds or faults), obtain
231 fracture statistics for discrete fracture models (Sect. 1.3), or test efficacy of forward geomechanical fracture models. For these
232 studies applied towards understanding deeper deformation, mineral filled fractures may be more useful or appropriate than focusing
233 solely on open fractures. Also, for deep-Earth applications, near-surface and geomorphology-related fractures are considered
234 “noise” and need to be omitted (e.g., Sanderson, 2016; Ukar et al., 2019). Yet, fractures that are noise to those interested in the
235 deep subsurface are essential features in the context of geomorphology and critical zone sciences. A major outstanding question is
236 how this differentiation might be reasonably and accurately accomplished given the relatively sparse number of studies of fractures
237 in the context of geomorphology. We hope future workers using this guide may find the answers.

238

239 1.3 Existing fracture modeling and statistics methods

240 Once fracture field data is collected, the metrics of its distribution can provide important insights into fracture processes (e.g.
241 Ortega et al., 2006). For example, power law distributions can be employed as a conservative rule of thumb for determining if

242 enough fractures have been measured (Sect. 4.2). Importantly, however, not all observations of fracture characteristics will be
 243 power-law distributed, with other heavy-tailed distributions possibly indicating other, less random controls on fracture properties;
 244 this is quite technical, and the reader is referred to Clauset et al (2009). If the data set is power-law distributed, however, then the
 245 power law exponent – the slope of the distribution in log-log plots—is the key parameter that determines the distribution of different
 246 fracture geometries. While it is tempting to just plot the data on a log-log plot and fit a line, this approach has proven to produce
 247 incorrect, strongly biased estimates. Again, without performing correct, unbiased statistical analysis, it is not possible to compare
 248 the power-law behavior and other statistics between different, carefully, and time-intensively collected data sets, limiting how
 249 generalizable the results are. It is an interesting and largely unaddressed question the extent to which they may be applicable in
 250 surface process-based fractures studies. Thus, for convenience, we outline the details of two straightforward, alternative approaches
 251 that have been developed for other, deeper-Earth applications that surface processes workers may test on their own data.

252 To understand fracture length and fracture width data, it is key to first recognize that, with the exception of studies such as in rocks
 253 with fractures with uniform spacing and bedding-controlled widths (Ortega et al., 2006), the data can commonly have a heavy-
 254 tailed distribution, such as lognormal, gamma, or power law. As mentioned above, of these, strong observational and theoretical
 255 evidence suggests that fracture size is commonly power law distributed (e.g., Bonnet et al., 2001; Davy et al., 2010; Hooker et al.,
 256 2014; Ortega et al., 2006; Zeeb et al., 2013), i.e.,

$$257 \quad n(b) = Ab^{-\alpha} \quad (1)$$

258 where b is the fracture dimension (length or width) of interest, n is the number of fractures with dimension d , and A and α are
 259 constants. When log-transformed, Eq. (1) becomes

$$260 \quad \log(n(b)) = \log(A) - \alpha \log(b) \quad (2)$$

261 which has led many practitioners to fit Eq. (2) by linearly binning the data in n , then log-transforming the data and fitting the
 262 resulting data with a linear regression. This has proven to lead to significant bias in estimates, $\hat{\alpha}$, of the power law exponent
 263 (Bonnet et al., 2001; Clauset et al., 2009; Hooker et al., 2014) and is not recommended despite its common usage.

264 Two straight-forward approaches have been shown not to have biases, or misestimates of the exponent α . 1) The following is based
 265 on Clauset et al. (2009). First, the exponent can be found from the cumulative distribution of the dimensions, $C(b)$, or number of
 266 fractures with dimension greater than b , i.e.,

$$267 \quad C(b) = \int_b^{b_{\max}} n(b) db \quad (3)$$

268 Where b_{\max} is the maximum size of the fracture dimension (e.g., maximum length or width). The cumulative power law distribution
 269 has the form

$$270 \quad C(b) \propto b^{1-\alpha} \quad (4)$$

271 It is common to denote $1-\alpha$ as c . To find α (or c), the dimension data is logarithmically binned. In other words, the dimension data
 272 is binned on a logarithmic (1, 10, 100, ...) frequency scale, and then log-transformed. At this point, linear regression techniques

273 can be applied to estimate α and assess uncertainty. However, in all cases, uncertainty estimates such as R^2 will overestimate the
274 certainty for such log-transformed data; but at least the estimate of α is unbiased.

275 2) Another method to find α from a data set of fracture dimensions is to use the maximum likelihood estimator (MLE) given by

$$276 \quad \hat{\alpha} = 1 + N \left[\sum_{i=1}^N \ln \left(\frac{b_i}{b_{\min}} \right) \right]^{-1} \quad (5)$$

277 where $\hat{\alpha}$ is the estimate of the exponent in (1), b_i is the dimension of the i th fracture, b_{\min} is the minimum valid fracture dimension
278 (see below) and N is the total number of samples (Clauset et al., 2009; Hooker et al., 2014). The MLE estimate has the advantage
279 of an accurate estimate of standard error, σ , given by

$$280 \quad \sigma = \frac{\hat{\alpha}-1}{N} + \mathcal{O}\left(\frac{1}{N}\right). \quad (6)$$

281 Clauset et al. (2009) showed that both the logarithmically-binned cumulative distribution and the MLE estimator produce unbiased
282 estimates of the exponent. For all empirical power law distributions, there is a scale; in this case b_{\min} , below which power law
283 behavior is not valid. This can be visually assessed by plotting Eq. 2 with logarithmically binned n . The interval between b_{\min} and
284 b_{\max} where the slope is linear is where the power law is valid (Clauset et al., 2009; Ortega et al., 2006), and Clauset et al. (2009)
285 presents a formal method to find b_{\min} and b_{\max} . Hooker et al. (2014) use a χ^2 test to evaluate the goodness of fit, which is simpler
286 than the p-tests of the Kolmogorov-Smirnov statistic proposed by Clauset et al. (2009).

287 2 Guiding Principles

288 2.1 Natural rock fracturing background

289 The design of any fracture-related study in the context of surface processes must arise from consideration of the variables that may
290 influence the rates of fracturing and the characteristics of the fractures that form. When rock is proximal to Earth's surface, those
291 variables include factors related to Earth's topography, atmosphere, biosphere, cryosphere, and/or hydrosphere. Here, a very brief
292 overview is provided of some key rock fracture mechanics concepts behind these factors. Eppes and Keanini (2017) and Eppes
293 (2022) provide more detailed reviews of rock fracture and fracturing processes in the context of surface processes.

294
295 Rocks fracture at and near Earth's surface in response to the complex sum of all tectonic (e.g., Martel, 2006), topographic (e.g.,
296 St. Clair et al., 2015; Moon et al., 2020; Molnar, 2004), biological (e.g., Brantley et al., 2017; Hasenmueller et al., 2017), and
297 environment-related (e.g., Matsuoka and Murton, 2008; Gischig et al., 2011) stresses they experience. Fracturing can occur when
298 stresses exceed the failure criteria (i.e., short-term material strength). More commonly, however, because critical stresses are rarely
299 reached in nature, fractures can also propagate *subcritically* at stresses as low or lower than 10% of the rock's strength (see
300 textbooks such as Schultz, 2019; Atkinson, 1987).

301
302 Overall, subcritical fracture propagation rates and processes are strongly dependent on stress magnitude, but they are *also* strongly
303 influenced by the size of the fracture that is under stress (see fracture mechanics textbooks such as Anderson, 2005; or reviews
304 such as Laubach et al., 2019). For single isolated fractures, stresses applied to the rock body are concentrated at fracture tips
305 proportional to the length of the fracture (a concept embodied by the term 'stress intensity'), effectively increasing the stresses

306 experienced by that fracture. Simultaneously, as the entire group of fractures within the rock body grows, the rock can become
307 ‘tougher’ – more resistant to further brittle failure under the same magnitudes of stresses, as the total rock mass becomes more
308 compliant (Brantut et al., 2012). Overall, the time-dependency of these interacting and contrasting behaviors is not well
309 characterized in natural settings - deep, shallow or surface.

310
311 In addition to fracture geometry, environmental conditions also strongly impact fracture tip bond breaking during subcritical
312 fracture. The environmental factors known to impact subcritical rock cracking - separate from their influence on stresses - include
313 vapor pressure, temperature, and pore-water chemistry (Eppes and Keanini, 2017; Eppes et al., 2020; Brantut et al., 2013; Laubach
314 et al., 2019). Therefore, in the context of surface processes, climate matters twice for rock fracturing: 1) as it contributes to the
315 stresses that the rock experiences, and 2) as it contributes to the chemo-physical processes that break bonds at fracture tips as they
316 propagate subcritically.

317
318 Just as other common physical properties like tensile strength can be measured, rocks can be tested for their propensity to fracture
319 subcritically by the measurement of subcritical cracking parameters such as the subcritical cracking index (e.g., Paris and Erdogan,
320 1963; Chen et al., 2017; Holder et al., 2001; Nara et al., 2012; Nara et al., 2017). These parameters influence both the rate of
321 subcritical cracking in rock and the fracture characteristics (e.g., amount of fracture per area or fracture length as in Olson, 2004).

322
323 In sum, natural rock fracturing is not necessarily the singular, catastrophic event, as it frequently portrayed in surface processes
324 research. Instead, it is likely dominantly a slowly evolving process progressing over geologic time as has been recognized from
325 fracture patterns in bedrock (e.g. Engelder, 2004; Rysak et al., 2022), and more recently in the context of surface processes
326 (Shaanan et al., 2023). Importantly, however, there is currently little field-based data elucidating these complex, experimentally
327 observed phenomena in surface processes contexts. It is therefore our hope that this guide will enable more workers to document
328 the complex feedbacks between rock and fracture properties, as well as environmental, topographic, and tectonic factors, that likely
329 influence all fracturing at and near Earth’s surface.

330 **2.2 Study design and site selection using a “State Factor” approach**

331 Due to their influence on rock fracturing as described above, all potential driving stresses and variations in fracture environments
332 must be considered in study design and site selection for any fracture-related research. Parent rock, topography (and other loads),
333 climate, biota, and time all potentially impact initiation and propagation of surficial fractures in rocks. Though this idea might
334 generally exist in other fracture-focused research, in the field of soil geomorphology it has long been explicitly described as a
335 ‘State Factor’ approach (e.g., Jenny, 1941; Phillips, 1989) to understanding progressive chemical and physical alteration processes.
336 Thus, we propose that this well-vetted conceptual paradigm may be employed in fracture-focused surface processes research as a
337 standard.

338
339 Here, it is asserted that applying a State Factor approach to fracture research is relevant because fracturing processes are influenced
340 by each of these factors, just as all other chemical processes acting on rock and soil. This is particularly true when the subcritical
341 nature of rock fracture is considered (Sect. 2.1). Thus, all State Factors that could contribute to fracture propagation styles, and
342 rates should be explicitly considered and controlled for as much as possible within the aims and scope of the research for any given

343 site. These ‘State Factors’ - long categorized as they relate to overall soil development, of which physical weathering is a
 344 component (e.g., Jenny, 1941) - are equally applicable to fractures alone, and include climate (cl, both regional climate and
 345 microclimate), organisms (o, flora and fauna), relief (r, topography at all scales), parent material (p, rock properties) and time (t,
 346 exposure age or exhumation rate). For rock fracture, tectonics (T) should be added to this list, making cl,o,r,p,t,T.

347
 348 Hereafter, the term ‘site’ refers to a single location of either a group of rock clasts or a group of outcrops, whereby all clasts or
 349 outcrops within the ‘site’ could be reasonably assumed to have experienced similar State Factors over their exposure history. For
 350 example, a site might comprise a single boulder bar on an alluvial fan surface or a single ridgeline with several outcrops. Once the
 351 specific State Factors (including the internal variability of each site) are identified for all the sites within a given field area, a series
 352 of sites can be selected whose State Factors are known and controlled for as much as possible. This enables a study of the influence
 353 of individual factors across the sites, i.e., fracture chronosequences, climosequences, toposequences, or lithosequences.

354
 355 For rock fracture, it is important to understand how each cl,o,r,p,t,T factor may contribute both to stresses that give rise to fracturing,
 356 and/or to the molecular-scale processes that serve to subcritically break bonds at fracture tips (Sect. 2.1). Based on existing
 357 experimental data and weathering research, and without evidence to show otherwise, we infer that each has the potential to
 358 independently impact fracturing rates, styles, and processes in surface processes contexts. The following descriptions provide only
 359 brief examples from that literature as to how each of the State Factors may influence rock fracture. To fully describe each of their
 360 influences on rock fracturing generally would comprise a textbook. Assuredly, to date, there are insufficient data to propose a
 361 hierarchy of their influence on fracture characteristics in surface processes contexts. The factors are therefore listed in the
 362 cl,o,r,p,t,T order by traditional convention only.

363 2.2.1 Climate (cl)

364 *Climate (cl)* as a State Factor refers not just to regional mean annual precipitation or temperature, but also the local microclimate
 365 of a site, which may be influenced by site characteristics, such as runoff or aspect. The presence of liquid water increases the
 366 efficacy of water-related stress-loading processes like those related to freezing (Girard et al., 2013) or chemical precipitation of
 367 salts or oxides (e.g., Buss et al., 2008; Ponti et al., 2021). Moisture – particularly vapor pressure – can also serve to accelerate rock
 368 fracturing rates independent of any stress-loading (e.g., Eppes et al., 2020; Nara et al., 2017). Temperature cycling can produce
 369 thermal stresses (through differential expansion and contraction of both adjacent minerals as well as different portions of the rock
 370 mass, e.g., Ravaji et al., 2019), and can also influence rates and processes of fracture-tip bond breaking (e.g., Dove, 1995).

371 2.2.2 Organisms (o)

372 *Organisms (o)* refers to both flora and fauna - everything from overlying vegetation and large animals to roots and microorganisms,
 373 all of which may provide a source of rock stress and/or may influence water availability or chemistry. These relationships can be
 374 complex and unexpected. For example, tree motion during wind and root swelling during water uptake both exert stresses on rock
 375 directly (Marshall et al., 2021a). Organism density and type can impact rock water and air chemistry (Burghelea et al., 2015), both
 376 of which may impact the rates and processes of subcritical cracking (e.g., review in Brantut et al., 2013).

377 2.2.3 Relief (r)

378 In the context of State Factors, *relief* (*r*) refers generically to all metrics related to topography including aspect, slope, and
 379 convexity. Topography impacts the manifestation of both gravitational stresses, as well as tectonic stresses within the rock body
 380 (Molnar, 2004; Moon et al., 2020; Martel, 2006). The directional aspect of a particular outcrop or boulder face may also influence
 381 insolation and water retention, translating into differences in microclimate and vegetation and, thus, weathering overall (e.g.,
 382 Burnett et al., 2008; West et al., 2014; Mcauliffe et al., 2022), including fracturing (e.g., West et al., 2014).

383 2.2.4 Parent material (p)

384 The *parent material* (*p*) factor in the context of a fracture study refers to the specific rock type(s) containing fractures (and
 385 potentially undergoing fracture) in the geomorphic environment. Rock varies in the types and dimensions of material present (e.g.,
 386 sandstone, siltstone, shale, basalt, granite etc.) and the types and spatial arrangements of interfaces within the material (e.g., grain
 387 size, porosity, bedding, foliation). These properties directly influence the rates and styles of fracture propagation (Atkinson, 1987)
 388 due to both how they respond to stresses but also due to how they allow stresses to arise (e.g. through their compliance, thermal
 389 conductivity, etc.). Thus, different rock properties differently influence the rates and characteristics of fracture growth and
 390 susceptibility to topographic and environmental stresses. For example, different minerals are characterized by different coefficients
 391 of thermal expansion. As a result, rocks with different mineral constituents will be more or less sensitive to thermal stresses than
 392 others depending on the contrasts between adjacent grains. Rock mineralogy will also impact chemical processes acting at crack
 393 tips during subcritical cracking, as well as the overall susceptibility of the rock to chemical weathering.

394
 395 Many (perhaps most) rocks contain fractures that formed prior to exposure, either due to deep seated tectonics and fluid pressure
 396 loads or to thermal and mechanical effect due to uplift towards the surface (English and Laubach, 2017; Engelder, 1993). In
 397 sedimentary rocks, fracture patterns (and, in some cases, fracture stratigraphy) vary with mechanical stratigraphy (e.g., Laubach et
 398 al., 2009) that can also influence near-surface fracture. In many instances, mechanical properties may be reflected in fracture
 399 stratigraphy, and vice versa. Schmidt hammer measurements are a useful, fast, and inexpensive field approach to documenting
 400 mechanical property variability (Aydin and Basu, 2005), however such measurements are impacted by weathering exposure age
 401 (e.g. Matthews and Winkler, 2022). The influence of fracture characteristics of the parent rock that may have formed in the deep
 402 subsurface are described in Sect. 2.2.6 “Tectonics”.

403
 404 Additionally, in the context of surface processes studies, we propose that parent material also refer to the size and shape of the
 405 clast or outcrop. Because, for example, angular corners generally concentrate stresses more than rounded edges (Anderson, 2005).
 406 Also, clasts or outcrops of different sizes experience different magnitudes of thermal stresses related to diurnal heating and cooling
 407 (Molaro et al., 2017).

408 2.2.5 Time (t)

409 *Time* (*t*) likely plays a role in rock fracturing rates just as it does in chemical weathering, whereby outcrops found in slowly-eroding
 410 environments or clasts on old surfaces may be subject to different fracturing rates and processes (e.g., Rasmussen et al., in review;
 411 Mushkin et al., 2014). Over time, rock mechanical properties can also change as weathering occurs (e.g., Cuccuru et al., 2012).
 412 Although the time factor has not been well-studied in the context of natural rock fracture, preliminary data suggest that it should

413 be considered (Berberich, 2020; Rasmussen et al., 2021). Published surficial geologic maps or datasets of rock exposure ages or
 414 erosion rates (e.g., Balco, 2020) can provide ‘time’ information.

415 2.2.6 Tectonics (T)

416 Finally, in a fracture-related study, *tectonic (T)* setting must also be considered as a State Factor. Fractures that have formed in the
 417 deep to near subsurface in response to tectonic forces such as plate-scale stress fields, folding, and faulting (and attendant pore
 418 pressure variations) may continue to propagate at or near the surface, and they inevitably become exhumed. Overall, fractures
 419 formed by these processes have traditionally been studied within the structural geology discipline, and that literature is extensive
 420 (e.g., reviews in Laubach et al., 2019; Laubach et al., 2018; Atkinson, 1987, Chapter 2). The tectonic history of rock can be recorded
 421 or manifest in its brittle structures that are then maintained over a wide range of past tectonic events, including its most recent
 422 exhumation and cooling. The attributes of resulting open or filled fractures depend on how deeply the material was buried, how
 423 rapidly uplifted, and the material properties (e.g., English and Laubach, 2017). Finally, the fact that the current tectonic setting can
 424 drive ongoing deformation has long been recognized (e.g., Hooke, 1972), and more recent work has highlighted that very low
 425 magnitude tectonic stresses can translate to fracture propagation in very near-surface bedrock, especially when interacting with
 426 local topography (e.g., Martel, 2011; Moon et al., 2020).

427
 428 It is likely, though perhaps not widely appreciated, however, that fractures originally opened due to tectonic stresses further
 429 propagate, not only due to ongoing tectonic stresses as they approach the surface, but also due to topographic and environmental
 430 stresses that the rocks increasingly encounter as they are exhumed to shallower depths. Simultaneously, these ‘new’ stresses may
 431 increase the overall number density (total number of fractures per area) and fracture intensity (defined here as total fracture length
 432 per area). These changes in fracture characteristics may manifest abruptly with depth or more gradually and those changes may
 433 manifest differently under different topographic portions of the landscape (e.g., ridges versus valleys). There is a growing body of
 434 data pointing to such surface interactions (e.g., Marshall et al., 2021b; Moon et al., 2019; Moon et al., 2020; St. Clair et al., 2015),
 435 but overall, these differentiations are a topic ripe for further study.

436
 437 Pre-existing fractures may not always be easily separable from those formed or further propagated under geomorphological
 438 influence. Environmental stresses also produce parallel fractures (e.g., Aldred et al., 2015; Eppes et al., 2010; Mcfadden et al.,
 439 2005), as do those related to the morphology of the eroding landscape (Leith et al., 2014). Thus, for outcrops, and particularly for
 440 clasts where correlations or comparison with regional tectonic structures are not possible, fracture orientations may not uniquely
 441 represent a tectonic regime. The non-geomorphic origin (or otherwise) of such fractures may be evident from microstructure
 442 analyses that examines fractures for diagenetic cements, inconspicuous mineral deposits, fluid inclusions, or other similar features
 443 (e.g., Ukar et al., 2019). Thus, in choosing study sites, consideration should be made of rock age, tectonic history and current
 444 tectonic setting (e.g., World Stress Map, Heidbach et al., 2018), as well as unambiguously tectonically-related structures such as
 445 dipping bedding planes, evidence of mineral deposits in the fractures, stylolites, or ductile structures such as folds (Hancock, 1985;
 446 Laubach et al., 2019).

447 2.3 Bedrock outcrops versus deposited clasts

448 The fracture characteristics of outcrops have long been employed as proxies for subsurface fracture networks, and there is a
 449 reasonably large body of literature addressing these relationships and their potential pitfalls (e.g., Ukar et al., 2019; Al-Fahmi et
 450 al., 2020; Sharifigaliuk et al., 2021). However, based on the growing body of research mentioned above, topographic and
 451 environmental stresses both have likely contributed to any sub-aerially observed fracture network unless otherwise ruled out. Thus,
 452 for studies that aim to isolate fractures associated with environmental stresses, measurements from clasts may be more useful than
 453 outcrops.

454
 455 Clasts that have been transported by fluvial, glacial, or mass-wasting processes have experienced abrasion, and therefore, it is
 456 highly likely that pre-existing superficial fractures have been removed. Thus, clasts may be more reasonably considered ‘fresh’
 457 than an outcrop with an unknown exhumation history, allowing clearer linkages between environmental exposure and observed
 458 fractures. This idea of “resetting” fractures within clasts through transport is supported by data showing clasts of identical rock
 459 type that have experienced more transport (i.e., rounded river rocks) having higher strength than those found in, for example, recent
 460 talus slopes (Olsen et al., 2020). Nevertheless, clasts may carry with them an invisible (to the unaided eye) population of pre-
 461 existing fractures— or sealed microfractures—that do in some instances impart a strength anisotropy that can manifest in later
 462 surface-related fractures, even in clasts. Thus, for such rocks, the ‘reset’ may be imperfect (e.g. Anders et al. (2014). In-depth
 463 petrographic analysis to identify residual microstructures (e.g. ala Forstner and Laubach, 2022) may not be feasible in most
 464 instances, but a simple uniaxial point load test, or field Schmidt-hammering of clasts found in active channels, may reveal if an
 465 inherited anisotropy is present.

466 **3 Selecting the clasts, outcrops, or rock surface locations that will comprise the fracture observation area**

467 Carefully selecting the rock surface area(s) on which fractures will be observed and measured within a site is equally as important
 468 as selecting the site or the fractures themselves. Hereafter, the term ‘observation area’ refers to the specific portion(s) of rock
 469 surface(s) for which fractures are being measured. Observation areas may comprise the entire exposed surface of individual clasts,
 470 outcrops, or portions of either (Fig. 1). In the following sections, instructions for selecting these observation areas in the field are
 471 provided.

472 **3.1 Establishing outcrop or clast selection criteria**

473 Before observation areas can be identified, outcrops or clasts must be selected. The first step of that selection process is to establish
 474 criteria for determining which outcrops or surface clasts within the site are acceptable for measurement. Without evidence to
 475 proceed otherwise, similar to site selection, variability in cl, o, r, p, t, T factors that may influence fracturing (temperature, moisture
 476 availability, rock shape, and rock type) should be controlled for as much as possible.

477
 478 In general, characteristics of the clasts or outcrops that might impact mechanical properties, moisture, or thermal stress-loading
 479 should be most heavily considered. The rock type properties that should be considered when developing selection criteria include
 480 not only heterogeneities like bedding or foliation, but also grain size and mineralogy, all of which can influence fracture rates and
 481 style characteristics. For example, perhaps only outcrops with no visible veins or dikes will be employed; or only outcrops greater
 482 than 1 m in height; or only north facing outcrop faces. Past work, for example, has focused on upward facing surfaces of outcrops
 483 or large clasts (e.g., Berberich, 2020; Eppes et al., 2018).

484

485 For loose clasts, only clasts of a particular size or rock type might be employed for measurement. For example, past work found
 486 that below approximately 5 cm diameter in semi-arid and arid environments (Eppes et al., 2010), and 15 cm in more temperate
 487 environments with vegetation (Aldred et al., 2015), clasts are more likely to have been moved or disturbed. Thus, these sizes were
 488 employed as a threshold for selection.

489 3.2 Non-biased selection of clasts or outcrops for measurement

490 Once criteria are defined, clasts or outcrops meeting those criteria must be randomly chosen for the fracture measurements. A
 491 procedure similar to the well-vetted Wolman Pebble Count style transect (Wolman, 1954) should be employed to avoid sampling
 492 bias. For landforms with other geometries, a grid may be used instead of a transect line.

493

494 In either case, a tape transect or net grid is laid out on the ground at each site, and the clast or outcrop closest to specified intervals
 495 on the tape (or at the points of the grid meeting the criteria) is selected (Fig. 1a). The interval or grid spacing should be adjusted to
 496 the overall size and abundance of clasts or outcrops found on the surface. If there are relatively few meeting the criteria at a site,
 497 all within the site meeting the criteria can be measured.

498

499 A similar technique can and should be applied for selecting outcrops. For example, care should be taken to not be limited to the
 500 'best' outcrops (cleanest and/or largest), since they likely are the least fractured. However, such large, clean outcrops may be the
 501 best places to observe any pre-existing subsurface-related fractures. For locations where outcrops are within a few meters or tens
 502 of meters of each other and vegetation relatively sparse, a grid of a set dimension (e.g., 100 m) is overlain on aerial imagery, and
 503 the closest outcrop to each grid intersection meeting the outcrop criteria are selected (Watkins et al., 2015). For areas where
 504 outcrops are not visible in aerial imagery, a measured or paced transect can be employed where the user walks along a bearing and
 505 chooses the closest outcrop meeting the selection criteria at each interval, e.g., 30 paces.

506

507 In all of the above, transect locations and orientations should be selected following consistent criteria and being mindful of the
 508 State Factors cl,o,r,p,t,T. For example, all transects or grids might be placed uniformly along backslopes with a certain upslope
 509 distance from the crest; or along the latitudinal center or crest of a landform. Alternatively, the transect might be orientated
 510 perpendicular or oblique to a paleo-flow direction so that it is not constrained only to bars or swales. The coordinates and bearing
 511 of all transects or grids should be recorded, enabling tracking and avoiding repetition.

512 3.3 Observation areas comprising the entire clast or outcrop surface

513 Fractures are three-dimensional objects, and ideally observations should encompass volumes; but, this is precluded by the opacity
 514 of rock, so one- or two-dimensional observation areas must be used. Fracture arrays may also encompass a wide range of sizes, so
 515 the selection of observation area(s) needs to consider truncation and censoring biases.

516

517 The observation area for small clasts and outcrops can be their entire exposed surface. In our experience, when clasts or outcrops
 518 selected for measurements are less than ~50 cm in maximum dimension, measurements can typically be readily made for all
 519 fractures visible on the clast or outcrop exposed surface for most rock types.

520

521 We strongly suggest that rocks should not be moved during measurement. This non-disturbance practice is particularly crucial for
 522 maintaining Earth's geodiversity (Brilha et al., 2018) and preserving sites for future workers to revisit. Further, research examining
 523 acoustic emission localization of rocks naturally fracturing found that the large majority of fracture 'foci' were located in the upper
 524 hemispheres of boulders (Eppes et al., 2016). Thus, we infer that the potential insight gained by moving clasts does not warrant
 525 the impact to geoheritage.

526 3.4 Establishing 'windows' as the observation area for larger clasts and outcrops

527 Particularly for larger exposures, it is not feasible to measure every fracture on an outcrop or clast. In these cases, the observation
 528 area may comprise predetermined 'windows' of representative decimeter- to meter-scale areas of the rock surface (Fig. 1b). This
 529 window selection method results in an accurate representation of fractures on an entire outcrop (e.g., Zeeb et al., 2013) and is least
 530 affected by some subjective biases (Andrews et al., 2019).

531

532 Importantly, the number and size of windows observed on each outcrop or at each site should depend on the typical number and
 533 size of fractures present on the surface of the rock (Sect. 4.2). Inevitably it is our experience that logistical constraints will dictate
 534 that decisions must be made about size cutoffs. Some part of the smallest size fraction of fractures may not be readily visible, and
 535 the finite size of exposures may mean that some large fractures are missed. Overall, it is preferable to strike a balance between
 536 window size and number so that during data analysis, variance can be quantified by comparing data collected between windows
 537 on the same outcrops and at the same site. More total observation area (e.g. more and/or larger windows) is required when fractures
 538 are fewer per area. The size of the area required for a representative quantification of fractures depends both on fracture average
 539 length and number density (e.g., Zhang, 2016). Here, an iterative approach is outlined for determining if sufficient area has been
 540 examined (Sect. 4.2), but other rules of thumb exist, particularly in the Rock Quality Designation Index literature (e.g., Zhang,
 541 2016).

542

543 Choosing the placement of windows on the outcrop should entail a stratified random sampling approach. Just as for clast- or
 544 outcrop-selection, cl,o,r,p,t,T factors like aspect should be taken into consideration and controlled for as much as possible in the
 545 window placement strategy by, for example, only using upward facing surfaces. Then, window placement determination is made
 546 to avoid sampling bias and edge effects. For example, if upward facing outcrop surfaces are to be characterized, then the total
 547 length and width of the face could be employed to align sufficient numbers of windows along even intervals of those measurements
 548 (e.g., three windows whose centers are located along the center axis of the rock with even spacing between the edges and each
 549 box; Fig. 1b).

550

551 For the placement of each window, it is our experience that a simple cardboard template of the appropriate window size with a
 552 center hole can be employed to trace with chalk the window directly on the clast or outcrop. Then, all fracture measurements are
 553 made in the window(s). Each window should be numbered and photographed in the context of each outcrop or clast. Also
 554 recommended is detailed photo-documentation of each outcrop and transect, along with sufficiently detailed coordinates to
 555 reoccupy the precise site (e.g. in meters or 0.00000 dd that are *always* referenced to the projection or datum used).

556 3.5 How many observation areas?

557 The number of clasts, outcrops, or windows required to measure sufficient fractures will vary with the study goals, site complexity,
 558 and the variables for which the data are being tested or controlled. Importantly, for each study, the required number of observation
 559 areas must be established based on the amount that is necessary to gain a statistically sufficient number of fracture observations to
 560 represent the rocks in question for that setting (Sect. 4.2). Concepts of ‘stationarity’ have been applied in the context of 2D analyses
 561 (e.g. Shakiba et al., 2023), but no rule-of-thumb in the context of surface processes is described herein because, as yet, there has
 562 not been sufficient standard fracture data collected to establish such a rule. Establishing such a rule of thumb is an illustration of
 563 the motivation of this paper, as well as an example of how the methods presented herein can and should evolve over time.

564
 565 Rocks or outcrops with lower fracture number density (fewer overall fractures per area) will require that larger areas of their surface
 566 be examined to measure sufficient fractures for statistical significance (Sects. 3.4 and 4.2). Rocks or outcrops with significant
 567 variation in fracture patterns require sufficient observation to capture that variability. Thus, as an example only, in past work, when
 568 State Factors were carefully controlled for, relationships between rock material properties and rock fracture properties were evident
 569 from about three to ten meter-scale outcrops per rock type on ridge-forming quartz rich rocks (Eppes et al., 2018). However, until
 570 sufficient magnitude of datasets have been collected for a particular site, the amount of observation area must be established based
 571 on the number of fractures available uniquely at each study site.

572 **4 Selecting fractures for measurement**

573 **4.1 Rules-based criteria for selecting fractures in surface processes research**

574 The term ‘fracture’ is employed with a wide variety of meaning across the geosciences, potentially resulting in large variations in
 575 the range of features that two individuals might study on a single outcrop (Long et al., 2019). Therefore, it is crucial to employ
 576 clear and repeatable rules-based criteria (e.g., Table 1) for what constitute measurable ‘fractures’ within any fracture-related
 577 research. Failing to do so consistently results in a high variance of subjective bias that is more reflective of worker personality than
 578 of the variance in fracture of the outcrop (Andrews et al., 2019). Thus, consistency and documentation are required for deriving
 579 interpretable and repeatable results.

580
 581 The proposed rules (Table 1) for determining which fractures to measure at any given field site were developed by us in the context
 582 of surface processes research and through iterations with numerous non-expert users (undergraduate students) to arrive at criteria
 583 that provided consistency in observations across users. Because surface processes are frequently and largely dependent both on
 584 rock erodibility and water within a rock body, the recommended criteria are applicable only to open voids, which are known to
 585 greatly impact both. Also, because other types of open voids like vesicles are common in rock, additional criteria includes that the
 586 open void must be planar in shape, bounded by parallel or sub-parallel sides (hereafter fracture ‘walls’), with a visible opening that
 587 is deeper than it is wide. Fracture walls commonly pinch together at fracture terminations.

588
 589 Voids that fit the shape criteria that are filled with lichens, dust, or other permeable material that can be readily brushed out with a
 590 fingernail or prodded with a needle should be included in the dataset. However, it is common for high length-to-aperture ratio
 591 voids in rock to have been filled with cemented mineral solids during intrusion and metamorphism, diagenesis, or weathering.
 592 Fractures, or portions of fractures containing these hardened cements, may become the hydrologic and mechanical equivalent of
 593 solid rock. Although such filled and partly filled fractures may be key to describing fractures formed in the deeper subsurface, we

594 assert that fully cemented fractures do not meet the defined ‘open’ criteria relevant to surface processes studies, and in principle
 595 should not be included in the fracture dataset. Where partly cement-filled fractures are present, specific rules may need to be
 596 adapted to account for the pattern of cement such as counting segments of fractures that are separated by continuous mineral
 597 deposits as separate features. If such a solid secondary mineral cement forms a discontinuous ‘bridge’ fully connecting the two
 598 walls of an otherwise open, planar void, the open length of the fractures on either side of the bridge would be treated as individual
 599 fractures. This partial ‘bridge’ or complete interruption of continuous fracture pore space is common in fractures that have existed
 600 at elevated temperatures such as at depth or near hydrothermal features (see review in Laubach et al., 2019), so a yes/no indication
 601 of their presence may be added to the dataset. A useful starting point for building such rules is to compare outcrops with
 602 expectations for how mineral deposits are typically configured in partly cemented fractures (e.g., Lander and Laubach, 2015).

603
 604 Finally, additional proposed criteria - based on our experience as well as fracture mechanics theory - is that the planar void must
 605 be continuously open (no ‘bridges’ of cemented mineral material or of rock) for a distance longer than 10 times the characteristic
 606 grain size dimension or 2 cm, whichever is greater. In most rock types, this translates to a 2 cm minimum cutoff for countable
 607 fractures (Fig. 2a; see Sect. 5.4.1 for measuring lengths). This proposed length threshold is based on three features. First, past work
 608 has demonstrated that deriving precise (repeatable) detailed information - other than length - for fractures <2 cm in length is
 609 challenging (e.g., Eppes et al., 2010). Second, temperature-dependent acoustic emission measurements (Wang et al., 1989; Griffiths
 610 et al., 2017) and theoretical arguments suggest that on single year time scales, fractures on single grain and smaller length scales
 611 exist in thermodynamic equilibrium, randomly opening and closing under constant redistribution of ubiquitous diurnal to seasonal
 612 thermal stresses within surface rocks. The approximate statistical mechanical ‘rule-of-ten’ states that well-defined equilibrium and
 613 nonequilibrium, continuum-scale properties, e.g., viscosity, density, stress and strain, each determined by myriad microscale
 614 random processes, are obtained on length scales approximately 10 times an appropriate molecular length scale, e.g., average atomic
 615 size or mean free path length between colliding (gas) molecules. This interpretation is consistent with recommendations for the
 616 number of grains the minimum diameter of a sample is for repeatable testing of continuous rock properties such as rock strength
 617 and elastic moduli (e.g., ASTM, 2017).

618
 619 Last, and practically, the high abundance of fractures below this cutoff significantly increases the time required for fracture
 620 measurement. If these smaller fractures are of interest, they can be characterized with photographic analysis (not covered herein)
 621 or subjected to semi-quantification via an index (Sect. 5.2).

622
 623 Importantly, in some applications, it may be appropriate that a larger minimum threshold in fracture length is chosen. However, in
 624 that case, fracture abundances in the rock will possibly dictate that significantly larger observation areas of the rock exposure need
 625 to be employed in order to obtain sufficient numbers of fractures to provide representative data (Sect. 4.2).

626
 627 Regardless of the threshold length chosen for the study, two adjacent fractures separated by intact rock or bridges of cement are
 628 considered two fractures, even if at a distance they appear to be continuous (Fig. 2b). This practice results in repeatable
 629 measurement between multiple workers and provides the most accurate representation of past fracture growth and fracture
 630 connectivity in the rock body.

631 4.2 Determining how many fractures to measure

632 Most published fracture-focused studies provide no justification for the number of fractures they measure, begging the question -
 633 is the dataset representative of the rock body? Studies of fracture statistics suggest a minimum of ~200 fractures (Baecher, 1983)
 634 per site (as defined herein). For workers and situations that require more nuance or for which there is not ample rock surface to
 635 examine, we recommend an iterative approach. It is a long-recognized concept in fracture and rock mechanics that fracture size
 636 distributions are highly skewed and can be characterized by scale-independent power law distributions (e.g., Davy et al., 2010;
 637 Hooker et al., 2014). Power law distributions cross multiple orders of magnitude in frequency and scale, requiring up to an order
 638 of magnitude more observations to significantly define than the other, more tightly defined distributions. Thus, the best practices
 639 to understand the commonly observed power-law distribution of fracture size can be leveraged in most cases to ensure that a
 640 representative fracture population has been measured in any given dataset (Ortega et al., 2006).

641
 642 Here, it is recommended that to fully characterize the fractures for any site(s), outcrop(s), or feature(s) of interest, sufficient
 643 numbers of fractures should be measured such that, if the fracture parameters are power-law distributed, a statistically robust
 644 power-law distribution (p-values <0.01) in fracture length or aperture can be estimated from the data. While other log-normal,
 645 exponential, and Weibull distributions have been proposed for various fracture datasets (e.g., Baecher, 1983), employing these
 646 distributions depends on preexisting knowledge of the expected dataset, the very data set in the process of being collected. Thus,
 647 unless there is prior documentation of fracture distributions at a particular site, the power law distribution should suffice, and, in
 648 any case, power law distributions require the most samples for significance compared to the other distributions.

649
 650 Thus, in practice, it will be an iterative process to determine the number of fractures required for any given dataset; but generally,
 651 on the order of 10^2 fractures are required (e.g., Zeeb et al., 2013) to reach a representative distribution (Fig. 3). When sufficient
 652 numbers of fractures have been measured to result in such a distribution, then it can be assumed that the population of measured
 653 fractures is representative of all fractures on the rock, outcrop, or group of rocks/outcrops with certain features. For example, if the
 654 goal of a study is to test the influence of rock type on fracture density, enough fractures must be measured to allow for a power-
 655 law distribution of fracture size for *each* of the rock types. That population of fractures can then be considered representative of
 656 the given rock type, and statistics on other fracture properties like width can also be reasonably interpreted as representative.

657
 658 If after ~200 fractures are measured the power law distribution is not met, then it is likely the dataset does not follow a power-law
 659 distribution and the number of measurements can be considered sufficient (Baecher, 1983). Some fracture arrays – particularly
 660 those formed at depth - have narrow (or ‘characteristic’) size distributions that are not well approximated by power laws (e.g.
 661 Hooker et al., 2013). Another exception to the scale independent power law rule of thumb may be if there are abundant fracture
 662 terminations in infilling material. In this case, the size of the fracture (as defined by Table 1) is dictated by the spacing of the filled
 663 material bridges. Thus, fracture sets in rocks that contain abundant varnish or secondary precipitates like calcium carbonate may
 664 not follow the power-law rule, and a threshold number of ~200 fractures per site should be employed.

665
 666 An example of what the iterative process might look like is found in Fig. 3. In this example, all fractures were measured on the
 667 surface of 15-50 cm diameter granitic clasts selected along transects across both a modern wash bar (with few overall fractures per
 668 clast) and a ~6 ka alluvial fan bar (with many fractures per clast). For the modern wash, after 5, 30, or 50 clasts, a statistically
 669 significant power law distribution is not evident (Fig. 3). However, after 130 clasts, the fit of the power law falls below a p-value

670 threshold of 0.01 with 111 fractures measured. Thus, measurements from around 130 clasts (~100 fractures) were necessary to
 671 fully characterize fractures for that particular site. In contrast, the threshold p-value is reached after only 5 clasts (64 fractures) for
 672 clasts with high fracture number density on the mid-Holocene age site; however, with more clasts examined, more variables per
 673 clast can be analyzed in the data. Thus, in order to evaluate different variables (like clast size or shape), the iterative process would
 674 repeat, but limiting the analysis to fractures found on clasts meeting the criteria of interest. In this example, a total of 130 clasts
 675 per surface were measured, enabling several subsets of data to be examined in order to test the influence on a range of clast
 676 properties on fracture characteristics. This iterative approach will give a reasonable assurance of when enough samples have been
 677 collected, but determining the type of distribution and estimating the distribution parameters, i.e., the exponent of the power-law,
 678 require more careful analysis that is covered below in section 6.

679 **5 Proposed baseline field data for fracture-focused surface processes research**

680 Here, a basic suite of field data (Table 2) is proposed for all observation areas and all fractures. Table 3 contains a list of
 681 recommended field equipment to make the measurements. The list of data in Table 2 was developed with the goal of allowing the
 682 worker to fully analyze their fracture data in the context of variables known from the literature to influence or reflect fracture in
 683 exposed rocks. Workers may choose to measure only some of these data if, for example, they have controlled for a particular metric
 684 through site or clast selection. As overall knowledge of fractures in surface environments grows, the suggested set of measured
 685 variables should also change, just as, for example, the components of the simple stream power equation have evolved in fluvial
 686 geomorphology literature. The proposed fracture field methods list is also focused on direct ‘observables’ – without interpretation
 687 – that should apply universally across field areas. We readily acknowledge that additional items can and should be added to
 688 accommodate the needs of any specific study.

689
 690 The metrics listed in Table 2, and the associated methods described below, are designed to be applicable and translatable to both
 691 natural outcrops and individual clasts. While they may also be applicable to fractures found in quarries and road-cuts, such outcrops
 692 are prone to fracturing that has been anthropogenically induced by blasting, exhumation, and new environmental exposure (e.g.,
 693 Ramulu et al., 2009; He et al., 2012).

694 **5.1 The ‘Fracture Sheet’**

695 A data collection template is provided that comprises all the proposed standard data, allowing efficient, complete, and detailed
 696 recording of all parameters while in the field (e.g., a “fracture sheet”, Fig. 4 with digital version provided in supplemental data).
 697 The fracture sheet can and should be modified to include additional parameters relative to any study. The template provided here
 698 is structured, based on our past experience, so that each observation area’s information (e.g., that of each clast, outcrop, or window)
 699 shares a row with the first fracture measured. Then, subsequent rows are employed for additional measured fractures on the same
 700 observation area. Each observation area and fracture are assigned unique identifiers to enable unambiguous reference in subsequent
 701 data analysis. Employing a ‘window’ rather than an entire clast or outcrop as the observation area necessitates slightly different
 702 data collection, so two separate fracture sheets can be found in the supplement.

703
 704 The fracture sheet provides a header space for site meta-data. Any observations that could elucidate the possible contributions of
 705 any State Factor (cl,o,r,p,t,T) acting at the site should be recorded (e.g., the vegetation or topography of the site). This header area

706 should also be employed to note any and all criteria or conventions used throughout the study. For example, the use of any
 707 convention, such as right-hand rule for strike and dip measurements, should be noted in the header. The criteria employed to select
 708 clasts or outcrops (e.g., their size, composition, etc.) and the nature of the observation areas (e.g., only the north face of all clasts;
 709 or entire exposed clast surface for all outcrops) should also be noted.

710 5.2 The use of semi-quantitative indices

711 It is recommended that indices be employed for many observations following similar existing semi-quantitative methods
 712 commonly employed in both soil sciences (e.g., Soil Survey Staff, 1999) and sedimentology (e.g., rounding and sorting). We have
 713 found in our experience that the use of indices, rather than precise measurements, is especially appropriate for fractures and fracture
 714 characteristics given the natural variation between different rocks. Also, high numbers of small or discontinuous features on rock
 715 surfaces frequently precludes their accurate counting within a reasonable amount of time; for example, counting all fractures <2
 716 cm in length.

717
 718 Two particularly useful generic ‘abundance’ indices are defined here that are derived from those employed for quantifying the
 719 abundance of roots and pores in soils (Schoeneberger et al., 2012), whereby the quantity or coverage of specific elements or features
 720 is estimated within a specified area. For both, a ‘frame’ is employed whose size is dependent on the size of the feature being
 721 observed (Fig. 5). Features that are ≤ 0.5 cm are observed in 1 cm² frames; features >0.5 to <2 cm are observed in a 10 cm² frame;
 722 and features ≥ 2 cm are observed in a m² frame. Cut-out stencils of these sizes may be constructed and employed. The observer
 723 imagines randomly placing the ‘frame’ several times on any given portion of the observation area, noting the abundance of the
 724 feature of interest within the frame. The indices are based on the average value of abundance observed in any given such ‘frame’
 725 across the entire area of observation (e.g., the entire clast, the entire outcrop, or the outcrop window).

726
 727 The first index scales from 0 to 4 and is applicable for ‘countable’ features of interest in the research like small fractures, fossils,
 728 or large phenocrysts. The index is: none – 0 (no visible features in any frame), few -- 1 (<1 feature on average), common -- 2 (≥ 1
 729 and <5 features on average), very common -- 3 (≥ 5 and <10 features on average), and many -- 4 (≥ 10 features on average).

730
 731 The second index scales from 0 to 5 and is employed for features that are not readily counted nor consistent in size (like lichen,
 732 varnish, fine grained mafic, or felsic minerals). In these cases, the index is based on the percentage of the rock surface covered by
 733 the feature: none – 0; very little – 1 ($<10\%$); little – 2 (≥ 10 and $<30\%$); common – 3 (≥ 30 and $<60\%$); very common – (≥ 60 and
 734 $<90\%$); and dominant – 5 ($\geq 90\%$). A percentage estimator (Fig. 6) should always be employed to assign the index categories –
 735 even experienced field workers are subject to ‘quantity bias’.

736 5.3 Measuring rock characteristics

737 The following rock characteristics are measured for each observation area – each clast, outcrop, and/or window – that is employed
 738 in a study. Some fracture characteristics not captured in individual fracture measurements are also included. In particular, fracture
 739 connectivity and fracture spacing should be measured after all individual fractures within the observation area have been identified
 740 and measured.

741 5.3.1 Clast, outcrop, or window dimensions

742 Rock – or outcrop – size, aspect, and slope can impact stress-loading through, for example, thermal stress distribution (e.g., Molaro
743 et al., 2017; Shi, 2011). Or, for instance, natural outcrop height has been linked to its exposure age and/or erosion rates (e.g.,
744 Hancock and Kirwan, 2007; Anderson, 2002). The dimensions of the clast, outcrop, or window employed for fracture observations
745 are also required for calculations of fracture number density and intensity (i.e., the number/length of fractures per unit area; see
746 Sect. 6.1).

747
748 The length and width of planar ‘windows’ are measured directly. If a window ‘bends’ across multiple faces of the rock surface,
749 then separate length and width measurements should be made for each face with a distinct aspect. These areas are then added
750 together for fracture number density and intensity calculations.

751
752 The vast majority of rock clasts and outcrops found in nature have ‘cuboid’ forms (Domokos et al., 2020). Thus, length, width,
753 and height of individual clasts or outcrops may be reasonably employed to calculate the exposed surface area (see Sect. 6.1 for
754 calculations). If clasts or outcrops are well-rounded, spherical or half-spherical surface areas can be employed, depending on burial.
755

756 For all dimension measurements regardless of rock shape, metrics are measured as point-to-point orthogonal measurements. By
757 convention, length is measured parallel to the longest axis. Width is measured on the widest extent that is perpendicular to length,
758 and height is measured vertically from the uppermost surface of the rock down to the ground surface. In past surface processes
759 work (e.g. Aldred et al., 2016; Eppes et al., 2010; McFadden et al., 2005), we have developed the rule of thumb that if a through-
760 going fracture splits the rock into two pieces that remain *in situ*, it should still be considered one rock and measured accordingly.
761 Such fractures formed in place, and provide information about the fracturing history of the rock (e.g. D’arcy et al., 2014). If a clast
762 or outcrop is spheroidal in shape, that should be noted for future surface area calculations.

763
764 For site preservation, and to minimize geoheritage and environmental impacts, we believe that rocks should not be moved from
765 their natural state; therefore, the height measurement of a highly embedded rock will only represent the height of the exposed rock
766 surface above the ground. A metric derived to estimate the degree to which clasts are exposed versus embedded is provided in
767 Sect. 5.3.8.

768 5.3.2 Sphericity and roundness

769 Sphericity and roundness from standard sedimentology practices (e.g., Krumbein and Sloss, 1951) provide metrics for rock shape.
770 Shape can influence stress distribution in a mass and, therefore, rock fracture. For example, generally, corners tend to concentrate
771 stresses, and ‘corner fractures’ are a recognized phenomenon in fracture mechanics (e.g., Kobayashi and Enetanya, 1976). Thus,
772 this metric has been included as one to be measured both for outcrops and for clasts.

773
774 Sphericity refers to the length by width ratio, or elongation, of the clast or outcrop, whereas roundness is a measure of angularity
775 (Fig. 7). The roundness and sphericity designation for the square on the chart in Fig. 7 most closely matching the dominant shape
776 of the entire clast or outcrop should be noted (ex. r-SR; s-SE). If a more precise rock shape analysis is needed, a modified Kirkbride
777 device can be used to quantitatively measure rock roundness (see Cox et al., 2018 for device modifications and methodology).

778 **5.3.3 Grain size**

779 Mean grain size can impact numerous fracture and stress characteristics including the proclivity for granular disintegration
 780 (Gomez-Heras et al., 2006), fracture toughness (Zhang et al., 2018), initial fracture length, thermal stress disequilibrium (Janio De
 781 Castro Lima and Paraguassú, 2004), and bulk elastic properties (Vazquez et al., 2015). The mean grain size is visually estimated
 782 by comparing the dominant size of individual grains or mineral crystals to a standard grain size card. This size can be reported as
 783 one average value for all minerals, or different values for different suites of minerals (e.g., felsic vs. mafic), depending on the
 784 lithological assemblage(s) of the observation area(s) and the goals of the study.

785 **5.3.4 Fabric and fracture filling**

786 Here, the term ‘fabric’ is employed to refer to any preexisting (prior to weathering) primary or diagenetic planar, linear, or randomly
 787 oriented anisotropies within the rock comprising the outcrop or clast of interest. Fabric is most commonly observed as fossils or
 788 lithological bedding planes in sedimentary rocks and as crystal horizons or foliation structures in igneous or metamorphic rocks.
 789 Also, all rocks can have diagenetic mineral deposits within parts of otherwise open fractures or contain fully filled veins and dikes.
 790 Finding mineral deposits in open fractures points to a deeper origin. Rock fabric can impart anisotropy that influences rock strength,
 791 fluid flow, and fracturing clustering, rates, and orientations (e.g., Nara and Kaneko, 2006; Zhou et al., 2022). Thus, any visible
 792 fabric type, as well as the strike(s) and dip(s) (or trend(s) and plunge(s)) of each parallel or subparallel set is noted in the fracture
 793 sheet for each observation area. Through comparison of orientations, it can be determined the extent to which fractures in the
 794 dataset are influenced by these fabrics.

795 **5.3.5 Fractures <2 cm in length**

796 Fractures <2 cm in length can comprise a significant portion of all fractures on a given rock exposure, particularly in coarse
 797 crystalline rock types (e.g., Alneasan and Behnia, 2021). Thus, it is recommended that an index is recorded (Sect. 5.2), using an
 798 observation ‘frame’ that quantifies the abundance of fractures less than 2 cm in length (hereafter ‘small fractures’). In our
 799 experience, this data can help to explain, for example, fracture densities that are lower than expected when derived from the >2 cm
 800 fracture length dataset alone.

801

802 The approximate number of small fractures visible each time the ‘frame’ is moved should be observed. A rough average of all
 803 theoretical frames should be taken, and the categories in Fig. 5 should be used to assign an abundance. For example, if there are
 804 generally either zero or one small fracture in any given 10 x 10 cm frame, the abundance would be “1” – i.e., few, <1 per unit area.

805 **5.3.6 Granular disintegration**

806 Granular disintegration refers to evidence of *active* loss of individual crystals or grains due to fracturing along grain boundaries
 807 (i.e., sedimentary particles or igneous or metamorphic crystals). This feature is observed on the rock surface as individual grains
 808 or small clusters of grains of the rock that can be brushed away by hand. Granular disintegration is commonly observed in coarse
 809 igneous, metamorphic, and sedimentary rocks, and over the long-term leads to the accumulation of ‘grus’ - sediment comprised of
 810 individual crystals or small clusters of a few crystals on the ground surface (Eppes and Griffing, 2010; Isherwood and Street, 1976;
 811 Gomez-Heras et al., 2006).

812

813 By necessity, this disintegration comprises the complete separation of intergranular fractures, and similar to fractures <2 cm, we
 814 have experienced that it can provide information about smaller scale fracturing of the rock (e.g. Eppes et al., 2018). Because the
 815 fractures that comprise granular disintegration are typically too small to be readily measured in the field, however, its presence is
 816 assumed when loose grains are present on the rock surface. The worker marks affirmatively (circling the ‘G’ on the Fracture Sheet)
 817 if there is evidence of granular disintegration on the rock surface of observation. If more detail is desired, an abundance index (e.g.,
 818 Fig. 5) may be employed to quantify what percentage of the surface of observation contains loose grains.

819 5.3.7 Pitting

820 Pitting is the occurrence of small holes or fissures that form on the rock surface due to granular disintegration or to preferential
 821 chemical weathering of certain mineral types, typically feldspars and micas in silicate rocks. Pitting is distinct from granular
 822 disintegration as it is not necessarily ‘actively’ occurring – i.e., pitting can exist without loose grains on the rock surface. It is
 823 included here as a rock property because of its possible linkage to intergranular fracturing. Furthermore, measuring the extent and
 824 depth of pitting due to chemical weathering has long been employed as a relative age dating tool in Quaternary geology applications
 825 (Burke and Birkeland, 1979).

826
 827 Pitted surfaces form as individual grains become weathered and fall out or are dissolved; or, for soluble rocks like carbonates, as
 828 entire rock regions are dissolved. Pitting is quantified either as present/absent (circling P on the fracture sheet) or as a quantity
 829 index (Figs. 4 and 5).

830 5.3.8 Clast exposure

831 This metric is used to record to what degree individual clasts appear to be exposed above the ground surface. Individual clasts are
 832 known to weather and erode from the upper rock surface down until they become ‘flat’ rocks at the ground surface (e.g. Ollier,
 833 1984), and the degree of embeddedness can impact preservation of fracture orientations (e.g. Aldred et al., 2015). We have found
 834 in our experience that surface exposure can be estimated as the amount and shape of a boulder’s exposed surface that is currently
 835 not covered by loose sediment, vegetation, or other material, and also relates to erosion rate in some settings. This exposure is
 836 grouped into four categories: 0 - the clast is sitting above the ground, and its sides curve downward toward the ground surface
 837 almost meeting; 1 - the clast is partially covered, with sides curving downward toward the ground surface but not meeting; 2 - the
 838 clast is “half” covered, with sides projecting roughly vertically into the ground surface; 3 - the clast has only one upward facing
 839 side visible at the ground surface. In a field study, a correlation test on data from 300 boulders revealed a positive correlation of
 840 0.66 between the indices and the fraction of boulder embeddedness (in vertical height) (Shaanan et al., 2022).

841 5.3.9 Lichen and varnish

842 Lichens and other plant life can act to push rocks apart during growth (Scarciglia et al., 2012), but have also been shown to
 843 strengthen rocks through infilling of voids or shielding from stress-inducing sunlight (Coombes et al., 2018). It is noted that lichen
 844 are living organisms that would be killed by removal. We have found that in order to determine if a lichen-coated lineation is in
 845 fact a measurable fracture (see Sect. 4.1), a large needle or straight pin may be employed to poke through the lichen into the
 846 possible void of the fracture.

847

848 Rock varnish (oxide staining that can appear as a dark gray/black or orange coating on rock and typically contains Fe or Mn oxides)
 849 is well-documented to evolve over time. The extent of varnish cover has been employed frequently as a relative-age indicator,
 850 particularly in arid environments (e.g., Mcfadden and Hendricks, 1985; Macholdt et al., 2018). Thus, we infer that variations in
 851 varnish across the rock face can provide evidence of loss of surface material through *in situ* fracturing.

852

853 Lichen and varnish can come in many forms and be difficult to distinguish from each other and from primary rock minerals, hiding
 854 in fractures, pitting holes, and atop mafic crystals. So, careful consideration of the types of lichen and varnish that may be found
 855 in field sites and close inspection with a hand lens is recommended. A fresher exposure of the rock surface can help in the
 856 identification of lichen and varnish relative to the natural rock composition and color. Due to the geodiversity impact, however,
 857 such exposures should not be made with force.

858

859 The quantity of lichen and varnish (secondary chemical precipitates deposited on the subaerial rock surface) visible on the rock
 860 observation surface are separately estimated using a visual percentage estimator (Fig. 6) and a quantity index is assigned (Fig. 5;
 861 Sect. 5.2).

862

863 5.3.10 Collecting samples for microfracture analyses

864 Rock microfractures (those not visible with hand lens in the field) play a central role in contributing to rock strength, anisotropy,
 865 and subsequent macrofracturing processes (Kranz, 1983; Anders et al., 2014). It is beyond the scope of the field-based methods
 866 presented herein to describe microfracture measurement and analysis, which continues to evolve (e.g., Griffiths et al., 2017; Healy
 867 et al., 2017). Instead, suggestions for rock sampling and placement of thin-section billets are provided.

868

869 Thin-section analysis of microfractures can be a time-consuming process, particularly when considering the per-capita rock volume
 870 examined. It is therefore extremely important to select rock or portions of rock that are precisely the rock type of interest, and to
 871 carefully orient the sample. For loose clasts, an entire clast can be sampled and a thin-section billet processed in the lab. For larger
 872 clasts and bedrock, a smaller portion must be extracted. By sampling pieces that are already naturally detached, or nearly detached,
 873 fracturing that arises due to chiseling or hammering is avoided. Epoxying samples prior to thin section preparation helps preserve
 874 delicate features and avoids introducing artifacts. Extra-thick sections are recommended for microfracture work, since conventional
 875 sections are prone to develop fractures during grinding. For population sampling, continuous sections can be created of any length
 876 (Gomez and Laubach, 2006).

877

878 For both clasts and outcrops, the natural orientation of the sampled rock (its horizontal and azimuthal directions) is always marked
 879 on the specimen. The sample should be photographed prior to removing from its location. It is essential to ensure all permitting is
 880 in place prior to sampling.

881

882 Similar to clast or outcrop selection, care must be taken when considering the location within the rock that the thin-section billet
 883 will be cut. Because microfracture strike and dip can be influenced by environmental, gravitational, and tectonic forces, both the
 884 depth and orientation of the billet should be noted and controlled for as appropriate for all samples compared within a single study.

885 5.3.11 Fracture connectivity

886 Fracture connectivity refers to the arrangement of fractures relative to each other and has long been recognized as being key to
 887 rock strength and fluid flow (e.g., Rossen et al., 2000; Long and Witherspoon, 1985; Manzocchi, 2002; Viswanathan et al., 2022),
 888 and presumably contributes to rock erodibility, given that fractures must intersect for rock to erode. There is a large body of
 889 literature that addresses fracture connectivity and how to measure it (e.g., Berkowitz, 2002; Barton et al., 1993; Healy et al., 2017;
 890 Sanderson and Nixon, 2018), especially in the context of reservoirs and rock quality index studies. As yet, fracture connectivity
 891 has been little studied in the context of surface processes, but likely holds high potential given its relationship to water access and
 892 to erodibility. Here, the focus is on a simple, rules-based observation of fracture intersection ‘nodes’ (e.g., Barton and Hsieh, 1989;
 893 Manzocchi, 2002; Forstner and Laubach, 2022; Sanderson and Nixon, 2018) that comprise the basis for fracture network
 894 connectivity assessment (e.g., Andresen et al., 2013).

895
 896 After all fractures within each observation area have been identified and measured (Sect. 5.4), all fracture links within the
 897 observation area should be counted and recorded by noting their relationship to other fractures (Fig. 8): dead end (I-node),
 898 crossing (X-node), and/or abutting without crossing (Y-node). Numbers of nodes per area can then be used as a proxy for
 899 fracture connectivity. If fracture connectivity is of particular interest for the research, rules-based ‘contingent mode’ (C-node)
 900 intersections may also be added (Forstner and Laubach, 2022). An example of a C-node rule might be if fractures >100 mm in
 901 length terminate within 10 mm of another fracture, its termination would be a c-node. Another C-node definition could comprise
 902 intersection relations where visible connected traces are sealed with secondary minerals. These c-nodes may be important when
 903 there are ambiguous at-depth relationships between fracture terminations (e.g., Fig. 2b).

904 5.3.12 Fracture spatial arrangement

906 In addition to overall fracture density, intensity and connectivity, the arrangement of fractures in space (e.g., evenly spaced,
 907 random, clustered in space) can impact loci of rock mass weakness, fluid flow, and landscape morphology. Laubach et al. (2018)
 908 comprises a special issue of the Journal of Structural Geology devoted to spatial arrangement of fractures, and much work has been
 909 published since. The mathematical analysis of spatial arrangement and rigorous identification of clustering is beyond the scope of
 910 this field guide. Freely available software is available for analyzing one-dimensional fracture arrangement along scan lines (Marrett
 911 et al., 2018) and for analysis of trace patterns in two dimensions (Corrêa et al., 2022; Shakiba et al., 2022).

912
 913 For scanline-based methods, following similar methods as those used for locating windows (Sect. 3.4), lines should be
 914 established across representative parts, or the center, of each observation area. For 1D analysis, good practice is to establish at
 915 least two perpendicular lines to capture different orientations of fractures, but the optimal number and configuration depends on
 916 the pattern under investigation. A tape or other linear measuring tool is then arranged along the lines, and, beginning with the
 917 edge of the observation area as distance 0, the distance along the tape of each fracture is noted (in other words, the sequence of
 918 spacing between fractures is recorded), with each measurement linked to the “Crack ID” already established for that fracture on
 919 the Fracture Sheet. If fractures are already marked with chalk, we find that this is an easy process. In that way, the size of each
 920 fracture and its adjacent distances are noted (analysis procedures allow weighting by fracture height, length, or aperture). As with
 921 any measure of fracture aggregate properties such as intensity or connectivity, for fractures having a wide range of sizes,

922 arrangement results depend on the size range of fractures included in the analysis (scale dependent) (e.g. Ortega et al., 2006).
923 These spatial arrangement data can go on the back of the Fracture Sheet.

924 5.4 Individual fracture characteristics

925 The following properties are measured for each fracture found within the observation area that meets all the fracture selection
926 criteria listed in Table 1. In order to keep track, we have found from experience that it is useful to mark fractures with chalk
927 within the observation area after you have made their appropriate measurements.

928 5.4.1 Length

929 Fracture length is measured for the entire surface exposure length of the fracture; i.e., around corners and up and down rock
930 topography (Fig. 2a). We have found these surface exposure distances to be the most repeatable and representative for the amount
931 of fracture exposed on the rock surface (Aldred et al., 2016). Measurements can be made with flexible seamstress tape to follow
932 the curve of a fracture's exposure on the rock surface. Length is only measured where there is an open void (Fig. 2b; Sect. 4.1),
933 because to measure across bridges of secondary cemented material or rock would be to infer future fracture propagation that has
934 not yet occurred. By only measuring the open portion of voids, the user avoids arbitrary interpretation of possible behavior. Thus,
935 if a seemingly continuous fracture (Fig. 2b, left inset) is in fact separated by bridges of solid rock (Fig. 2b, right inset), then these
936 should be measured as two different fractures and their lengths should terminate at the rock bridges (Sect. 4.1). The inset in Fig.
937 2b reveals four fractures possibly meeting all Table 1 criteria. If two fractures intersect in x- or y-nodes (Fig. 8), each fracture is
938 defined by its own distinct strike, and the full length of the full open fracture with that strike is measured (e.g., the length of
939 segments ab and cd in Fig. 8).

940
941 Importantly, when using a 'window' approach to rock observation area, both the total length of the fracture extending beyond the
942 window, as well as the total length within the window, should both be recorded. The latter is employed in fracture intensity
943 calculations (Sect. 6.1); the former provides representative information about all fracture lengths on the rock being measured.

944 5.4.2 Width

945 Fracture aperture widths (hereafter, 'widths') can impact both the strength and permeability of rock. Generally, they scale with
946 fracture length and, thus, can possibly reflect the innate subcritical cracking parameters of the rock (Olson, 2004). Fracture widths
947 typically vary along their exposure and pinch out at fracture tips. Determining an average or representative width within a single
948 fracture can thus be somewhat arbitrary and subject to bias. Locating the widest aperture is less subject to bias and can also provide
949 information about fracturing processes (for example, the widest aperture in a series of mechanically interacting en echelon fractures
950 should be in the center fracture; Anderson, 2005). Also, we find that the center of the open fracture is an objectively repeatable
951 location, and also where the fracture might be expected mechanistically to be the widest. However, given that this relationship can
952 become complicated as fractures fill or branch, unless there is reason to do otherwise, we recommend the rule of thumb to record
953 fracture width both at the midpoint of the measured length of the exposed fracture as well as at its maximum width along its
954 exposure.

955

956 We assert that in order to delineate the fracture – as opposed to measuring subsequent weathering or erosion - width measurements
 957 should only be made in regions of the fracture where fracture walls are parallel or sub-parallel (e.g., green arrows in Fig. 9),
 958 avoiding locations where fracture edges have been obviously rounded by erosion or chemical weathering, or where large pieces
 959 have been chipped off or are missing (e.g., red arrows in Fig. 9). If it is unclear if a portion of the fracture has chipped off (e.g.,
 960 orange arrow in Fig. 9), a notation can be made and employed later to eliminate potential outliers in the dataset. Fractures greater
 961 than about 3 mm in width can be easily measured by inserting the back-blades of digital calipers into the widest opening of the
 962 fracture. For narrower fractures, a logarithmically binned ‘crack comparator’ (Fig. 7) is recommended (Ortega et al., 2006),
 963 whereby the line on the comparator most closely matching the fracture aperture is chosen.

964 5.4.3 Strike and dip

965 Fracture orientation (i.e., strike and dip) is a function of the orientation of existing anisotropy within the rock and the orientation
 966 of the principal stresses that drove its propagation (e.g., Anderson, 2005). Fracture orientations are commonly related to tectonic
 967 forces; however, both gravitational and environmental stresses can also be directional (e.g., St. Clair et al., 2015; Mcfadden et al.,
 968 2005). When fractures are growing at subcritical rates, they can lengthen through a series of ‘jumps’ that link parallel or subparallel
 969 smaller fractures (e.g., Ma et al., 2023). The following suggestions are for research aimed, not at characterizing these small mm-
 970 cm scale heterogeneities, but rather identifying major stresses and heterogeneity in the entire rock body.

971
 972 Fracture orientation is measured with a geological compass or similar tool that has both azimuthal direction and inclinometer
 973 functionality. When measuring strike and dip of fractures, we find it is helpful to visualize how the fracture plane intersects the
 974 rock surface, as if slipping a sheet of paper into the ‘file folder’ of the fracture. For larger fractures, weathering and erosion may
 975 have resulted in loss of rock along the upper edge of the fracture, so it is imperative to measure the angle at the interior of the
 976 fracture where its walls are parallel (Fig. 9) to avoid measuring instead the angle of the eroded face.

977
 978 Fractures grow until they intersect other fractures and/or branch segment and link. If fractures appear to intersect, branch or link
 979 (i.e., two connected planar voids with noticeably different orientations joined by a sharp angle), their lengths should be measured
 980 separately as well as their orientations (e.g., two strikes and dips) as previously mentioned. This phenomenon is in some cases
 981 evident in 2D spatial analysis that takes length scales into account (e.g., Corrêa et al., 2022). For fractures that meander around
 982 mm-cm scale heterogeneities like phenocrysts or fossils, the overall trend is measured. A 1 to 10 rule of thumb (Sect. 4.1) can be
 983 used whereby, as long as the ‘jog’ in the fracture orientation is $<1/10$ of the fracture length, it is not measured.

984
 985 Fracture tip propagation direction may also slowly change as the orientation of external stresses or internal stress concentrations
 986 change within the rock mass. For curvilinear fractures, the average orientation can be measured, as the orientation of the non-
 987 curved plane whose ends are defined by the ends of the fracture. Alternatively, the fracture curvilinear plane may be subdivided
 988 into roughly linear planes and each orientation measured. If this latter approach is taken, the intersection should be marked as a
 989 node, and two lengths recorded. It is important to note which method was employed and to remain consistent for all measurements,
 990 as no widely acknowledged rule of thumb exists to our knowledge for this measurement.

991

992 There are numerous commonly-employed conventions for measurements of strike and dip. If the worker is consistent and clear in
 993 the use of their preferred convention and in the presentation of their data, any are acceptable. If the worker has no such prior habits,
 994 we recommend, from our experience, that to record strikes as an azimuthal orientation from 0-359 degrees, and dip angle as an
 995 angle deviation from horizontal of 0-90 degrees makes data analysis easier than recording, for example, direction by quadrant. For
 996 dip direction, we recommend a convention such as the “right-hand rule” be employed whereby the dip direction is always known
 997 from the orientation of the strike alone. For example, the right-hand rule states that the down-dip direction is always to the “right”
 998 of the measured and recorded strike when the observer is facing the same direction of the strike. Therefore, the strike that is
 999 recorded is the one whereby the dip direction is always +90 degrees clockwise (to the right) from the strike direction.

1000 5.4.4 Fracture parallelism

1001 Noting the parallelism of the fractures can help to better understand the origins of the population of fractures at a site. Parallelism
 1002 is common because fractures often follow rock heterogeneities or anisotropies such as bedding, foliation, veins, or even the rock
 1003 surface (e.g. McFadden et al., 2005). Fractures in a single bedrock outcrop or clast are also commonly parallel because they have
 1004 formed due to external stress-loading with a consistent orientation (e.g., those influenced by regional tectonics or directional
 1005 insolation). Thus, noting parallelism may help to distinguish the origins of fractures, though not always. For example, ‘surface
 1006 parallel fractures’ (e.g., Fig. 2a) - commonly referred to as exfoliation, sheeting joints (e.g., Martel, 2017), or spalling – vary
 1007 dramatically in scale and can have origins related to several different factors including tectonic-topographic interactions (Martel,
 1008 2006), chemical weathering and volumetric expansion (Røyne et al., 2008), and thermal stresses related to insolation (e.g., Lamp
 1009 et al., 2017; Collins and Stock, 2016) and fire (e.g., Buckman et al., 2021). Likewise, fractures having a strong preferred orientation
 1010 parallel to topographic features like escarpments or stream channels may predate the topography and have localized the geomorphic
 1011 feature, or they may postdate the feature and themselves be a response to topographic loads (e.g. Molnar, 2004). For this reason,
 1012 fracture pattern sampling that seeks to avoid or characterize these effects should include exposures distant from such ambiguous
 1013 situations (i.e., close to and distant from topographic features).

1014
 1015 In the fracture sheet, features to which the fracture is parallel should be documented. We find that a visual inspection will suffice
 1016 for most applications, but for applications where more precision is needed, the fracture may be considered parallel if the strike and
 1017 dip of a fracture is within $\pm 10^\circ$ of the orientation of the feature (the rock’s long axis, its fabric, or its outer surface). We base this
 1018 cutoff on the $\pm 4-7^\circ$ strike and dip orientation precision of a typical Brunton compass under ideal measuring conditions (e.g.
 1019 Whitmeyer et al., 2019). A fracture may be parallel to more than one feature in the rock. Categories may be added as necessary for
 1020 rocks with other repeating features unique to the field site (fossils; veins, etc.). Assertions of parallelism (or similar) are a potential
 1021 source of ambiguity, so careful consistency in the quantification of the basis of the claim is needed.

1022 5.4.5 Sheet height

1023 Surface parallel fractures naturally detach ‘sheets’ of rock between the fracture and the rock surface (‘h’ in Fig. 2a). Sheet height
 1024 is thus only measured for surface parallel fractures. We infer that the thickness of these sheets may be of interest for understanding
 1025 the size of sediment produced from the fracture or for understanding the stresses that produced the fracture. We provide the rule
 1026 of thumb that sheet height is measured using calipers at the location of the maximum height of the sheet, because thin edges often
 1027 break off and vary. To limit these measurements to those that have likely formed in situ as related to the current morphology of

1028 the rock, another rule of thumb we have employed is to only measure those ‘sheets’ that would result in removal of <10% from
 1029 the outer surface of the rock downward into the dimension(s) of the rock face(s) to which they are perpendicular.

1030 5.4.6 Weathering index

1031 Rock fracture is ultimately a molecular scale bond-breaking process; so, when fractures propagate, they initially form a razor-sharp
 1032 lip or edge where their two planes intersect the rock surface. Over time, these edges naturally round through subsequent chemical
 1033 and physical weathering, erosion, and abrasion (e.g., regions of the red arrows in Fig. 9). Crack tips may also blunt through time,
 1034 but that observation may be complicated by the presence of mineral deposits. Following similar research that has demonstrated
 1035 time-dependent changes in rock surface morphology due to such weathering processes (e.g., Shobe et al., 2017; Gómez-Pujol et
 1036 al., 2006; McCarroll, 1991), we established an index of relative degree of such rounding along a fracture edge (rather than crack
 1037 tip) to be noted in the fracture sheet:

- 1038
 1039 1: fresh with evidence of recent rupture (flakes/pieces still present, but not attached)
 1040 2: sharp, no rounded edges anywhere
 1041 3: mostly sharp with occasional rounded edges
 1042 4: mostly rounded edges with occasional sharp edges
 1043 5: all rounded edges
 1044

1045 6 Suggestions for data analyses

1046 When the data collection has been completed, it is necessary to provide statistics. For initial data exploration, general properties
 1047 may be calculated for rock and fracture data like the mean, median, variance, skewness, kurtosis, and overall ‘appearance’ of
 1048 distributions. Data can be compared using normal cross-plots, or quantile-quantile plots, as well as standard correlation analysis.
 1049 For categorical data, normal analytical techniques (histograms, discrete correlation analysis, etc.) can be applied. As with all heavy-
 1050 tailed data, the median is preferred over the mean value to understand a characteristic value—though power distributed data
 1051 generally does not have a characteristic dimension. Distribution characterization is discussed in section 1.3. 2D spatial analysis
 1052 methods can also be applied to entire outcrops or clasts, or to subdivisions of these features (Corrêa, et al., 2022; Shakiba et al.,
 1053 2023). These methods are well suited to large outcrops and well exposed fracture arrays.

1054 6.1 Fracture number density and fracture intensity

1055 Here, following large portion of fracture mechanics literature and for clarity, the term ‘fracture number density’ is employed to
 1056 refer to the number of fractures per unit area (e.g., # fractures/m²), and the term ‘fracture intensity’ to the sum length of all fractures
 1057 per unit area (e.g., cm/m²). However, it is crucial to note that these terms are frequently defined differently and in inconsistent
 1058 ways across disciplines and even within disciplines (e.g., Barthélémy et al., 2009; Narr and Lerche, 1984; Ortega et al., 2006;
 1059 Dershowitz and Herda, 1992). To avoid confusion, it is imperative that workers clearly define their usage in each work. In
 1060 particular, fracture intensity is scale dependent. If the outcrops or clasts on which fractures are measured vary greatly in size,
 1061 intensity calculations that account for the fracture distribution may be appropriate (e.g. Ortega et al., 2006).
 1062

1063 In the suggested simple use herein, the ‘area’ refers to the surface area of observation area. For fractures measured in ‘windows’
 1064 (Sect. 3.4), the length of fractures only *within* the window is used, and the area of the window (e.g., 10 cm x 10 cm) for the

1065 calculations. For loose clasts and outcrops, the appropriate calculation of surface area will depend on the shape and angularity of
 1066 the rock. For most rocks, calculations for the surface area of the exposed sides of a rectangular cuboid ($L*W + 2*(L*H) +$
 1067 $2*(W*H)$) are appropriate.

1068 6.2 Circular data

1069 Standard ‘linear’ statistics cannot be employed for circular data. Instead, circular statistical and plotting software is used for the
 1070 visualization and analysis of strike and dip data. The statistics employed by such software is typically based on established circular
 1071 statistical research methods (e.g., Mardia and Jupp, 1972; Fisher, 1993). The following statistics are from that work and are useful
 1072 in reporting strike and dip data.

1073
 1074 The Mean Resultant Direction (a.k.a. vector mean, mean vector) is analogous to the slope in a linear regression. Circular variance
 1075 can be quantified using either a Rayleigh Uniformity Test (for single mode datasets) or a Rao Spacing Test (for datasets with
 1076 multiple modes), whereby p-values <0.05 indicate non-random orientations. If p-values for these tests are below a threshold (e.g.,
 1077 <0.05), then data are considered non-uniform or non-random.

1078
 1079 The Rayleigh statistic is based on a von Mises distribution (i.e., a normal distribution for circular data) of data about a single mean
 1080 (i.e., unimodal data). Therefore, for multi-modal data, the variance might be high, but nevertheless, the data might be non-uniform.
 1081 The Rayleigh Uniformity Test calculates the probability of the null hypothesis that the data are distributed in a uniform manner.
 1082 Again, this test is based on statistical parameters that assume that the data are clustered about a single mean.

1083
 1084 Rao's Spacing Test is also a test for the null hypothesis that the data are uniformly distributed; however, the Rao statistic examines
 1085 the spacing between adjacent points to see if they are roughly equal (random with a spacing of $360/n$) around the circle. Thus,
 1086 Rao's Spacing Test is appropriate for multi-modal data and may find statistical significance where other tests do not.

1087 8 Case example

1088 Here we present a simple, brief example of how the presented methods promote consistency of results across users in fracture
 1089 measurements; to provide a full case study is beyond the scope of this paper. We provided minimal training (one demonstration
 1090 with some minor oversight of initial work) to four groups of two students each. The fifth pair of workers included a scientist who
 1091 had logged over 500+ hours of experience using the standardized methods. Each of the five groups followed the methods to
 1092 measure the length and abundance of fractures on boulders (15-50 cm max diameter) on the same geomorphic surface (a 6000-
 1093 year-old alluvial fan in Owens Valley California, comprised of primarily granitic rock types). Each group followed the methods
 1094 described herein for rock and fracture selection and measurements. As such, the results from each group (Fig. 10; Data Supplement)
 1095 could be compared not only for fracture selection and measurements, but also for observation area selection – a key component of
 1096 collecting data that is representative of a particular site.

1097
 1098 We find that the data collected by each of the groups for fracture length, number of fractures per rock, and rock size are statistically
 1099 indistinguishable by student t-test (all pairs of p-values > 0.1 ; Fig. 10; Data Supplement). Also, there is no consistent difference
 1100 between measurements made by the novice groups and that of the trained group. The mean fracture lengths from the four novice

1101 groups novice group (37 ± 23 mm to 59 ± 51 mm) span across that of the mean collected by the well-trained group (42 ± 22 mm;
1102 Supplement), as do the number of fractures per rock (2 ± 2 to 6 ± 8 for novice groups compared to 3 ± 3 for trained group). With only
1103 one exception (fracture length for Group 1), variance between groups does not range by more than a factor of 3 in any of the data
1104 – a common rule of thumb for the threshold of ‘similar’ variance between small datasets. Overall, especially given the relatively
1105 small size of the datasets (~10-20 rocks and ~40-60 fractures each), this comparison suggests that the results using the standardized
1106 methods are reproducible, even with novice workers with minimal training. A full case study and analysis would be required to
1107 fully and quantitatively evaluate all of the procedures presented herein.

1108 9 Conclusions

1109 The methods proposed herein comprise a ‘first stab’ at standardization of field data collected in rock fracture research surrounding
1110 surface processes and weathering-based geologic problems. The outlined methods comprise best practices derived in large part
1111 from existing work in the context of structural geology and geotechnical engineering. They also comprise general guidance and
1112 nuances developed from experiences (and mistakes) over the last two decades of fracture-focused field research applied to
1113 geomorphology and soil science. We readily acknowledge that additional, fewer, or altered methods may be appropriate for some
1114 applications. Nevertheless, it is our hope that providing these rules-based, detailed, accessible, standardized procedures for
1115 gathering and reporting field-based fracture data will open the door to rapidly building a rigorous galaxy of new datasets as these
1116 guidelines and methods become more widely adopted. In turn, they may enable future workers to better compare and merge fracture
1117 data across a wide range of studies. Doing so will permit future refinements not only of the methods themselves, but most
1118 importantly of our understanding of rock fracture. Compiling such a standardized global dataset is the best hope for fully
1119 characterizing the role and nature of fractures in Earth surface systems and processes.

1120 10 Author Contributions

1121 MCE spearheaded the evolution of the development of the guiding principles and methods described herein as well as writing of
1122 the manuscript. AR and SL contributed significantly to the editing of the manuscript’s content and expanding the breadth and depth
1123 of its applicability and approaches. JA, SB, MD, SE, FM, SP, MR, and US all participated extensively in field campaigns during
1124 which the methods were developed and refined, and they contributed to editing of manuscript and editing and development of
1125 figures. MM, AR and RK contributed to the development of theoretical statistical analyses practices that are outlined in the
1126 document and the editing of the manuscript.

1127 11 Competing interests

1128 The authors declare that they have no conflict of interest.

1129

1130 12 Data Availability

1131

1132 All data presented in the manuscript are available in the Supplement.

1133 13 Acknowledgements

1134 The body of knowledge presented herein was derived in large part over the course of research funded by the National Science
1135 Foundation Grant Nos. EAR#0844335 (with supplements #844401, #0705277), #1744864, and NSF-BSF #1839148 and NASA
1136 ROSES Mars Data Analysis Program award #NNX09AI43G. Several photographs in figures were cropped and employed with
1137 permission from Marek Ranis, Artist-in-Residence for NSF #1744864. We thank Claire Bossennec and Colin Stark for their
1138 constructive reviews. In addition, the authors wish to acknowledge the contributions from countless undergraduate and graduate
1139 students who contributed to the application and development of these methods in classes taught by MCE at the University of North
1140 Carolina at Charlotte.
1141
1142
1143

Figure Captions

Fig. 1. Images illustrating the selection of observation areas for clasts and outcrops. A. Photograph of a transect established for clast selection. Black dot: predefined transect interval location on the tape. Red dot: clast that does not fit the predefined clast selection criteria (e.g., it is too big). Green dot with red circle: clast that fits criteria but is further away from the interval point than the clast with the green dot. Green dot: closest clast to the transect interval that meets the selection criteria. B. Annotated photograph showing an idealized placement of ‘windows’ (dashed black squares) on a bedrock outcrop. Outcrop dimensions are measured and the windows are placed using predetermined selection criteria. In this example, the windows are equally spaced along the centerline of the long-dimension of the upward-facing side of the outcrop.

Fig. 2. A. Example of the measurement of a surface exposure length (L; yellow line) of a fracture meeting the criteria in Table 1. The ‘h’ refers to the location where sheet height would be measured for this surface parallel fracture. B. Example of fractures that may appear to be a single fracture (left), but upon close examination are in fact multiple fractures intersecting and/or separated by rock (right inset). Arrow points to the location of the inset image on the main image. Compass in the foreground for scale.

Fig. 3. Example histograms and statistics of fracture length data measured on the exposed surfaces of clasts 15-50 cm max diameter. Upper row are data for clasts found on a modern ephemeral stream boulder bar. Clasts overall have very low fracture number density. Lower row are data for clasts on an ~6 ka surface where fracture number density is much higher. Note that it takes about 100 clasts to arrive at a statistically significant power law distribution for the Modern Wash clasts, but only 5 rocks for the rocks with higher fracture densities. Producing histograms interactively as data is collected can help establish how many observation areas are necessary for a given site.

Fig. 4. Reduced size image of an 8.5” x 11” ‘fracture sheet’ to be employed in the field to increase efficiency and to reduce ‘missing’ data. Sheet templates for both clasts and outcrops that can be modified are provided in Data Supplement as well as a data-entry template.

Fig. 5. Visual aid for estimating the abundance of “countable” rock features – including fractures. An index of 0-4 is assigned depending on the abundance of features within an average of any given observation area (ex: 10 x 10 cm) on the clast or window being examined. The area of observation is defined by the size of the features being measured. A 10 cm x 10 cm square is used for estimating the abundance of ‘fractures < 2 cm’ defined as fractures with lengths of >0.5 cm but < 2 cm (see section 5.2 for details of how to use the index). For features ≤ 0.5 cm, a 1 cm x 1 cm area would be employed and for features ≥ 2 cm, a 1 x 1 m area. Ensure the image is printed to scale prior to use in the field.

Fig. 6. A visual percent estimator (modified from Terry and Chilingar, 1955). Estimator should be employed in every estimate of percentages. See section 5.2 for using the estimator to assign a percent coverage index to features that are not countable or vary in size (e.g., lichen coverage, fine mafic minerals, etc.).

Fig. 7. **Inset:** Roundness and sphericity chart – modified from Krumbein and Sloss (1951) to add the roundness and sphericity lettering. **Roundness:** A = angular; SA = subangular; SR = subrounded; R = rounded; WR = well-rounded. **Sphericity:** S = spherical; SS = subspherical; SE = sub-elongate; E = elongate. **Edges:** fracture comparator whereby the width most closely matching the fracture aperture is noted. Note: a to-scale pdf is available in the Data Supplement, however, owing to printing and publication scaling, it is highly recommended to calibrate the comparator prior to using it in the field.

Fig. 8 Depiction of types of fracture intersection nodes. I-nodes comprise fracture terminations with no connections. Y-nodes are abutting fractures that do not cross. X-nodes are fractures that cross. C-nodes are ‘contingent nodes’ defined by the user. In this example the rule is related to the distance between I-nodes. For #1, the distance is wider than the criteria, so the terminations are designated as I-nodes. For #2, the distance is within the limits, and the ‘connection’ is designated as a C-node.

Fig. 9. Examples of aperture transects that are appropriate for measurement of fracture aperture widths (green) and transects where there is evidence that the fracture walls have been eroded or chipped and therefore should not be employed for a width

1194 measurement (red). In cases where it is not clear if erosion or chipping has occurred (orange), a note can be made for the fracture
1195 width to possibly eliminate outliers during data analysis.
1196
1197
1198 Fig. 10. Box and whisker plots of case example data collected by five different pairs of workers on the same geomorphic surface.
1199 "x"s mark the means. Groups 1-4 were novice workers. Group 5 comprised one experienced worker. A. Fracture lengths B.
1200 Fractures per rock C. Clast length
1201

1202

1203 *Table 1. List of proposed rule-based criteria for defining measurable fractures*

<p>The answer to the following questions must be ‘yes’ for all measured fractures. Measure all fractures meeting these criteria within the observation area.</p>	<p><u>NOTES</u></p>
<ul style="list-style-type: none"> • Is the feature a lineament longer than it is wide? • Does the lineament contain open space bounded by walls? • If the lineament is not open, can the infilling material (ex: dust and lichens) be readily scraped out? • If the lineament is open or after the material has been scraped out, is the opening deeper than it is wide <u>and</u> bounded by ~parallel walls? • Is the open portion of the lineament ≥ 2 cm (>10 grains) in length (without interrupting bridges of rock or cemented infilling material)? 	<p>Do not measure:</p> <ul style="list-style-type: none"> • Spherical pores/vesicles. • Lineaments, or portions of lineaments, with solid mineral infilling/cement. • Ledge edges or linear etchings. • rock bridges between fractures

1204

1205 *Table 2. List of proposed data to collect for the rock observation area and for all fractures ≥ 2 cm in length*

<p>Rock Observations</p>	<p>Individual Fracture Observations</p>
<ul style="list-style-type: none"> • Dimensions of the observation area (e.g. clast, outcrop, and/or window length, width, height) • Rock type • Grain size • Mineralogy % (minimally felsic vs. mafic) • Sphericity of exposure • Roundness of exposure • Fabric description, strike, and dip (e.g. vein, foliation, bedding) • Granular Disintegration • Pitting • Lichen and Varnish • Fracture Connectivity • Fracture Spacing 	<ul style="list-style-type: none"> • Length (surface exposure length measured with a flexible tape) • Aperture width: center and maximum widths measured with calipers and/or comparator • Strike 0-360° (right-hand rule preferred) • Dip 0-90° • Parallelism (note features parallel to the fracture such as fabric, rock faces) • Sheet height (the thickness of what would be the detached spall or sheet of rock above a surface parallel fracture) • Weathering Index

1206

1207

1208

1209

Table 3. List of field equipment

<p>Required</p>	<p>Recommended</p>
<ul style="list-style-type: none"> • Hand lens (large, 10x) • Grain size card • Fracture comparator (for fracture widths) • Flexible seamstress tape measure (with mm) • Calipers (mm 0.0 to 150) • Brunton or similar compass • Roundness and sphericity chart • Visual percentage estimator • Fracture sheets 	<ul style="list-style-type: none"> • Camera with macro lens • Chalk for marking measured fractures and windows • Safety pin or needle for fracture exploration • Cardboard cutout frames for windows • Small white board or chalk board for including observation area ID in photos

1210

1211

1212 Bibliography

- 1213** Aich, S. and Gross, M. R.: Geospatial analysis of the association between bedrock fractures and vegetation in an arid environment, **1214** *International Journal of Remote Sensing*, 29, 6937-6955, 10.1080/01431160802220185, 2008.
- 1215** Al-Fahmi, M. M., Hooker, J. N., Al-Mojel, A. S., and Cartwright, J. A.: New scaling of fractures in a giant carbonate platform **1216** from outcrops and subsurface, *Journal of Structural Geology*, 140, 104142, <https://doi.org/10.1016/j.jsg.2020.104142>, 2020.
- 1217** Aldred, J., Eppes, M. C., Aquino, K., Deal, R., Garbini, J., Swami, S., Tuttle, A., and Xanthos, G.: The influence of solar-induced **1218** thermal stresses on the mechanical weathering of rocks in humid mid-latitudes, *Earth Surface Processes and Landforms*, 41, 603- **1219** 614, 2015.
- 1220** Alneasan, M. and Behnia, M.: An experimental investigation on tensile fracturing of brittle rocks by considering the effect of grain **1221** size and mineralogical composition, *International Journal of Rock Mechanics and Mining Sciences*, 137, 104570, **1222** <https://doi.org/10.1016/j.ijrmmms.2020.104570>, 2021.
- 1223** Anderson, R. S.: Modeling the tor-dotted crests, bedrock edges, and parabolic profiles of high alpine surfaces of the Wind River **1224** Range, *Wyoming Geomorphology* 46, 35-58, 2002.
- 1225** Anderson, T. L.: *Fracture Mechanics: Fundamentals and Applications*, Third, Taylor & Francis Group, Boca Raton, FL, 2005.
- 1226** Anders, M. H., Laubach, S. E., and Scholz, C. H., : Microfractures: a review. *Journal of Structural Geology*, 69, Part B, 377-394. **1227** doi: 10.1016/j.jsg.2014.05.011, 2014.
- 1228** Andresen, C. A., Hansen, A., Le Goc, R., Davy, P., and Hope, S. M.: Topology of fracture networks, *Frontiers in physics*, 1, 7, **1229** 10.3389/fphy.2013.00007, 2013.
- 1230** Andrews, B. J., Roberts, J. J., Shipton, Z. K., Bigi, S., Tartarello, M. C., and Johnson, G.: How do we see fractures? Quantifying **1231** subjective bias in fracture data collection, *Solid Earth*, 10, 487, 2019.
- 1232** ASTM: D7012-14: Standard Test Methods for Compressive Strength and Elastic Moduli of Intact Rock Core Specimens Under **1233** Varying States of Stress and Temperatures, 2017.
- 1234** Atkinson, B. K.: *Fracture Mechanics of Rock*, Academic Press Geology Series, Academic Press Inc., Orlando, Florida, **1235** <https://doi.org/10.1016/C2009-0-21691-6>, 1987.
- 1236** Ayatollahi, M. R. and Akbardoost, J.: Size and geometry effects on rock fracture toughness: Mode I fracture, *Rock Mechanics and **1237*** *Rock Engineering*, 47, 677-687, 10.1007/s00603-013-0430-7, 2014.
- 1238** Aydin, A. and Basu, A.: The Schmidt hammer in rock material characterization, *Engineering Geology*, 81, 1-14, **1239** <https://doi.org/10.1016/j.enggeo.2005.06.006>, 2005.
- 1240** Baecher, G. B.: Statistical analysis of rock mass fracturing, *Journal of the International Association for Mathematical Geology*, 15, **1241** 329-348, 10.1007/BF01036074, 1983.
- 1242** Balco, G.: Technical note: A prototype transparent-middle-layer data management and analysis infrastructure for cosmogenic- **1243** nuclide exposure dating, *Geochronology*, 2, 169-175, <https://doi.org/10.5194/gchron-2-169-2020>, 2020.
- 1244** Barthélémy, J.-F., Guiton, M. L. E., and Daniel, J.-M.: Estimates of fracture density and uncertainties from well data, *International **1245*** *Journal of Rock Mechanics and Mining Sciences*, 46, 590-603, <https://doi.org/10.1016/j.ijrmmms.2008.08.003>, 2009.
- 1246** Barton, C. C. and Hsieh, P. A.: *Physical and Hydrologic-Flow Properties of Fractures: Las Vegas, Nevada - Zion Canyon, Utah - **1247*** *Grand Canyon, Arizona - Yucca Mountain, Nevada, July 20-24, 1989 (Field Trip Guidebook T385)*, American Geophysical Union, **1248** Washington, D.C.1989.
- 1249** Barton, C. C., Larsen, E., Page, W. R., and Howard, T. M.: Characterizing fractured rock for fluid-flow, geomechanical, and **1250** paleostress modeling: Methods and preliminary results from Yucca Mountain, Nevada, United States, Medium: ED; Size: 74 p., **1251** 10.2172/145208, 1993.
- 1252** Bell, F.G.: *Engineering Geology*, 2nd edition. Butterworth-Heinemann Press, Burlington, MA, USA. 581 p. ISBN 978-0-7506- **1253** 8077-6. 2007.
- 1254** Berberich, S.: *A chronosequence of cracking in Mill Creek, California*, Geography and Earth Sciences, The University of North **1255** Carolina Charlotte, ProQuest, 2020.
- 1256** Berkowitz, B.: Characterizing flow and transport in fractured geological media: A review, *Advances in Water Resources*, 25, 861- **1257** 884, [https://doi.org/10.1016/S0309-1708\(02\)00042-8](https://doi.org/10.1016/S0309-1708(02)00042-8), 2002.

- 1258** Betlem, P., Birchall, T., Lord, G., Oldfield, S., Nakken, L., Ogata, K., and Senger, K.: High resolution digital outcrop model of faults and fractures in caprock shales, Konusdalen West, central Spitsbergen, Earth Syst. Sci. Data Discuss. [preprint], **1259** <https://doi.org/10.5194/essd-2022-143>, in review, 2022.
- 1260**
- 1261** Birkeland, P. W.: Soils and Geomorphology, Oxford University Press, New York, New York, 1999.
- 1262** Bonnet, E., Bour, O., Odling, N. E., Davy, P., Main, I., Cowie, P., and Berkowitz, B.: Scaling of fracture systems in geological **1263** media, Reviews of Geophysics, 39, 347-383, 2001.
- 1264** Borg, I. and Handin, J.: Experimental deformation of crystalline rocks, Tectonophysics, 3, 249-367, [https://doi.org/10.1016/0040-1951\(66\)90019-9](https://doi.org/10.1016/0040-1951(66)90019-9), 1966. **1265**
- 1266** Brantley, S. L., Eissenstat, D. M., Marshall, J. A., Godsey, S. E., Balogh-Brunstad, Z., Karwan, D. L., Papuga, S. A., Roering, J., **1267** Dawson, T. E., Evaristo, J., Chadwick, O., McDonnell, J. J., and Weathers, K. C.: Reviews and syntheses: On the roles trees play **1268** in building and plumbing the critical zone, Biogeosciences, 14, 5115, 2017.
- 1269** Brantut, N., P. Baud, M. J. Heap, and Meredith, P. G.: Micromechanics of brittle creep in rocks, J. Geophys. Res. 117, B08412, **1270** doi:10.1029/2012JB009299, 2012.
- 1271** Brantut, N., Heap, M. J., Meredith, P. G., and Baud, P.: Time-dependent cracking and brittle creep in crustal rocks: A review, **1272** Journal of Structural Geology, 52, 17-43, 2013.
- 1273** Brilha, J., Gray, M., Pereira, D. I., and Pereira, P.: Geodiversity: An integrative review as a contribution to the sustainable **1274** management of the whole of nature, Environmental Science & Policy, 86, 19-28, <https://doi.org/10.1016/j.envsci.2018.05.001>, **1275** 2018.
- 1276** Buckman, S., Morris, R. H., and Bourman, R. P.: Fire-induced rock spalling as a mechanism of weathering responsible for flared **1277** slope and inselberg development, Nature Communications, 12, 2150, 10.1038/s41467-021-22451-2, 2021.
- 1278** Burghelea, C., Zaharescu, D. G., Dontsova, K., Maier, R., Huxman, T., and Chorover, J.: Mineral nutrient mobilization by plants **1279** from rock: influence of rock type and arbuscular mycorrhiza, Biogeochemistry, 124, 187-203, 10.1007/s10533-015-0092-5, 2015.
- 1280** Burke, R. M. and Birkeland, P. W.: Reevaluation of multiparameter relative dating techniques and their application to the glacial **1281** sequence along the eastern escarpment of the Sierra Nevada, California, Quaternary Research, 11, 21-51, 10.1016/0033-5894(79)90068-1, 1979. **1282**
- 1283** Burnett, B. N., Meyer, G. A., and McFadden, L. D.: Aspect-related microclimatic influences on slope forms and processes, **1284** northeastern Arizona, Journal of Geophysical Research: Earth Surface, 113, <https://doi.org/10.1029/2007JF000789>, 2008.
- 1285** Buss, H. L., Sak, P. B., Webb, S. M., and Brantley, S. L.: Weathering of the Rio Blanco quartz diorite, Luquillo Mountains, Puerto **1286** Rico: Coupling oxidation, dissolution, and fracturing, Geochimica et Cosmochimica Acta, 72, 4488-4507, 2008.
- 1287** Chen, X., Eichhubl, P., and Olson, J. E.: Effect of water on critical and subcritical fracture properties of Woodford shale, Journal **1288** of Geophysical Research: Solid Earth, 122, 2736-2750, <https://doi.org/10.1002/2016JB013708>, 2017.
- 1289** Chilton, K. D. and Spotila, J. A.: Preservation of Valley and Ridge topography via delivery of resistant, ridge-sourced boulders to **1290** hillslopes and channels, Southern Appalachian Mountains, U.S.A., Geomorphology, 365, 107263, **1291** <https://doi.org/10.1016/j.geomorph.2020.107263>, 2020.
- 1292** Clauset, A., Shalizi, C. R., and Newman, M. E. J.: Power-law distributions in empirical data, SIAM review, 51, 661-703, **1293** 10.1137/070710111, 2009.
- 1294** Collins, B. D. and Stock, G. M.: Rockfall triggering by cyclic thermal stressing of exfoliation fractures, Nature Geoscience, 9, 395- **1295** 401, 2016.
- 1296** Coombes, M. A., Viles, H. A., and Zhang, H.: Thermal blanketing by ivy (*Hedera helix* L.) can protect building stone from **1297** damaging frosts, Nature: Scientific Reports, 8, 1-12, 2018.
- 1298** Corrêa, R. S. M., Marrett, R., and Laubach, S. E.: Analysis of spatial arrangement of fractures in two dimensions using point **1299** process statistics, Journal of Structural Geology, 163, 104726, <https://doi.org/10.1016/j.jsg.2022.104726>, 2022.
- 1300** Cox, R., Lopes, W. A., and Jahn, K. L.: Quantitative roundness analysis of coastal boulder deposits, Marine Geology, 396, 114- **1301** 141, <https://doi.org/10.1016/j.margeo.2017.03.003>, 2018.
- 1302** Cuccuru, S., Casini, L., Oggiano, G., and Cherchi, G. P.: Can weathering improve the toughness of a fractured rock? A case study **1303** using the San Giacomo granite, Bulletin of Engineering Geology Environments, 71, 557-567, 2012.

- 1304** D'Arcy, M., Roda Boluda, D. C., Whittaker, A. C. & Carpineti, A.: Dating alluvial fan surfaces in Owens Valley, California, using weathering fractures in boulders, *Earth Surface Processes and Landforms* 40, 487-501, 2014.
- 1306** Davy, P., Le Goc, R., Darcel, C., Bour, O., de Dreuzy, J. R., and Munier, R.: A likely universal model of fracture scaling and its consequence for crustal hydromechanics, *Journal of Geophysical Research: Solid Earth*, 115, <https://doi.org/10.1029/2009JB007043>, 2010.
- 1307**
- 1308**
- 1309** Deere, D.U.: Technical description of cores for engineering purposes. *Rock Mechanics and Engineering Geology*, 1, 18-22, 1964.
- 1310** Dershowitz, W. S. and Herda, H. H.: Interpretation of fracture spacing and intensity, *The 33rd U.S. Symposium on Rock Mechanics (USRMS)*, 1992.
- 1311**
- 1312** DiBiase, R. A., Rossi, M. W., and Neely, A. B.: Fracture density and grain size controls on the relief structure of bedrock landscapes, *Geology*, 48, 399-402, 2018.
- 1313**
- 1314** Domokos, G., Jerolmack, D. J., Kun, F., and Torok, J.: Plato's cube and the natural geometry of fragmentation, *Proceedings of the National Academy of Sciences*, 117, 18178-18185, 2020.
- 1315**
- 1316** Dove, P. M.: Geochemical controls on the kinetics of quartz fracture at subcritical tensile stresses, *Journal of Geophysical Research*, 100, 349-359, 1995.
- 1317**
- 1318** Engelder, T.: *Stress Regimes in the Lithosphere*, Princeton University Press, 1993.
- 1319** Engelder, T.: Tectonic implications drawn from differences in the surface morphology on two joint sets in the Appalachian Valley and Ridge, Virginia, *Geology*, 32(5), 413-416, 2004.
- 1320**
- 1321** English, J. M. and Laubach, S. E.: Opening-mode fracture systems: insights from recent fluid inclusion microthermometry studies of crack-seal fracture cements, *Geological Society, London, Special Publications*, 458, 257-272, doi:10.1144/SP458.1, 2017.
- 1322**
- 1323** Eppes, M.-C., 2022. Mechanical Weathering: A Conceptual Overview. In: Shroder, J.J.F. (Ed.), *Treatise on Geomorphology*, vol. 3. Elsevier, Academic Press, pp. 30–45. <https://dx.doi.org/10.1016/B978-0-12-818234-5.00200-5>.
- 1324**
- 1325** Eppes, M. C. and Griffing, D.: Granular disintegration of marble in nature: A thermal-mechanical origin for a grus and corestone landscape, *Geomorphology*, 117, 170-180, 2010.
- 1326**
- 1327** Eppes, M. C. and Keanini, R.: Mechanical weathering and rock erosion by climate-dependent subcritical cracking, *Reviews of Geophysics*, 55, 470-508, 2017.
- 1328**
- 1329** Eppes, M. C., McFadden, L. D., Wegmann, K. W., and Scuderi, L. A.: Cracks in desert pavement rocks: Further insights into mechanical weathering by directional insolation, *Geomorphology*, 123, 97-108, 2010.
- 1330**
- 1331** Eppes, M. C., Magi, B., Scheff, J., Warren, K., Ching, S., and Feng, T.: Warmer, wetter climates accelerate mechanical weathering in field data, independent of stress-loading, *Geophysical Research Letters*, 47, 1-11, 2020.
- 1332**
- 1333** Eppes, M. C., Magi, B., Hallet, B., Delmelle, E., Mackenzie-Helnwein, P., Warren, K., and Swami, S.: Deciphering the role of solar-induced thermal stresses in rock weathering, *GSA Bulletin*, 128, 1315-1338, 2016.
- 1334**
- 1335** Eppes, M. C., Hancock, G. S., Chen, X., Arey, J., Dewers, T., Huettenmoser, J., Kiessling, S., Moser, F., Tannu, N., Weiserbs, B., and Whitten, J.: Rates of subcritical cracking and long-term rock erosion, *Geology*, 46, 951-954, 2018.
- 1336**
- 1337** Fisher, N. I.: *Statistical Analysis of Circular Data*, Cambridge University Press, Cambridge, England, <https://doi.org/10.1017/CBO9780511564345>, 1993.
- 1338**
- 1339** Forstner, S. R. and Laubach, S. E.: Scale-dependent fracture networks, *Journal of Structural Geology*, 165, 104748, <https://doi.org/10.1016/j.jsg.2022.104748>, 2022.
- 1340**
- 1341** Girard, L., Gruber, S., Weber, S., and Beutel, J.: Environmental controls of frost cracking revealed through in situ acoustic emission measurements in steep bedrock, *Geophysical Research Letters*, 40, 1748-1753, 10.1002/grl.50384, 2013.
- 1342**
- 1343** Gischig, V. S., Moore, J. R., Evans, K. F., Amann, F., and Loew, S.: Thermomechanical forcing of deep rock slope deformation: 1. Conceptual study of a simplified slope, *Journal of Geophysical Research*, 116, 10.1029/2011JF002006, 2011.
- 1344**
- 1345** Glade, R. C., Shobe, C. M., Anderson, R. S., and Tucker, G. E.: Canyon shape and erosion dynamics governed by channel-hillslope feedbacks, *Geology*, 47, 650-654, 10.1130/G46219.1, 2019.
- 1346**
- 1347** Gomez, L. A., and Laubach, S. E.: Rapid digital quantification of microfracture populations, *Journal of Structural Geology*, 28, 408-420, 2006.
- 1348**

- 1349** Gomez-Heras, M., Smith, B. J., and Fort, R.: Surface temperature differences between minerals in crystalline rocks: Implications for granular disaggregation of granites through thermal fatigue, *Geomorphology*, 78, 236-249, 2006.
- 1350**
- 1351** Gómez-Pujol, L., Fornós, J. J., and Swantesson, J. O. H.: Rock surface millimetre-scale roughness and weathering of supratidal Mallorcan carbonate coasts (Balearic Islands), *Earth Surface Processes and Landforms*, 31, 1792-1801, <https://doi.org/10.1002/esp.1379>, 2006.
- 1352**
- 1353**
- 1354** Griffiths, L., Heap, M. J., Baud, P., and Schmittbuhl, J.: Quantification of microcrack characteristics and implications for stiffness and strength of granite, *International Journal of Rock Mechanics and Mining Sciences*, 100, 138-150, <https://doi.org/10.1016/j.ijrmms.2017.10.013>, 2017.
- 1355**
- 1356**
- 1357** Hancock, G. S. and Kirwan, M.: Summit erosion rates deduced from ¹⁰Be: Implications for relief production in the central Appalachians, *Geology*, 35, 89-92, 10.1130/g23147a.1, 2007.
- 1358**
- 1359** Hancock, P. L.: Brittle microtectonics: Principles and practice, *Journal of Structural Geology*, 7, 437-457, [https://doi.org/10.1016/0191-8141\(85\)90048-3](https://doi.org/10.1016/0191-8141(85)90048-3), 1985.
- 1360**
- 1361** Handin, J. and Hager, R. V., Jr.: Experimental deformation of sedimentary rocks under confining pressure: Tests at room temperature on dry samples, *AAPG Bulletin*, 41, 1-50, 10.1306/5ceae5fb-16bb-11d7-8645000102c1865d, 1957.
- 1362**
- 1363** Handin, J. and Hager, R. V., Jr.: Experimental deformation of sedimentary rocks under confining pressure: Tests at high temperature, *AAPG Bulletin*, 42, 2892-2934, 10.1306/0bda5c27-16bd-11d7-8645000102c1865d, 1958.
- 1364**
- 1365** Handin, J., Hager Jr, R. V., Friedman, M., and Feather, J. N.: Experimental deformation of sedimentary rocks under confining pressure: Pore pressure tests, *AAPG Bulletin*, 47, 717-755, 1963.
- 1366**
- 1367** Hasenmueller, E. A., Gu, X., Weitzman, J. N., Adams, T. S., Stinchcomb, G. E., Eissenstat, D. M., Drohan, P. J., Brantley, S. L., and Kaye, J. P.: Weathering of rock to regolith: The activity of deep roots in bedrock fractures, *Geoderma*, 300, 11-31, <https://doi.org/10.1016/j.geoderma.2017.03.020>, 2017.
- 1368**
- 1369**
- 1370** Hatir, M. E.: Determining the weathering classification of stone cultural heritage via the analytic hierarchy process and fuzzy inference system, *Journal of Cultural Heritage*, 44, 120-134, <https://doi.org/10.1016/j.culher.2020.02.011>, 2020.
- 1371**
- 1372** He, M., Xia, H., Jia, X., Gong, W., Zhao, F., and Liang, K.: Studies on classification, criteria, and control of rockbursts, *Journal of Rock Mechanics and Geotechnical Engineering*, 4, 97-114, 10.3724/SP.J.1235.2012.00097, 2012.
- 1373**
- 1374** Healy, D., Rizzo, R. E., Cornwell, D. G., Farrell, N. J. C., Watkins, H., Timms, N. E., Gomez-Rivas, E., and Smith, M.: FracPaQ: A MATLAB™ toolbox for the quantification of fracture patterns, *Journal of Structural Geology*, 95, 1-16, <https://doi.org/10.1016/j.jsg.2016.12.003>, 2017.
- 1375**
- 1376**
- 1377** Heard, H. C.: Effect of large changes in strain rate in the experimental deformation of Yule Marble, *The Journal of Geology*, 71, 162-195, 1963.
- 1378**
- 1379** Hencher, S.: *Practical Engineering Geology*. Spon Press, New York, NY, USA. 450 p. ISBN 97800-203-89482-8. 2015.
- 1380** Hencher, S.: *Practical Rock Mechanics*. Spon Press, New York, NY, USA. 356 p. ISBN 978-1-4822-1726-1. 2019.
- 1381** Heibach, O., Rajabi, M., Cui, X., Fuchs, K., Müller, B., Reinecker, J., Reiter, K., Tingay, M., Wenzel, F., Xie, F., Ziegler, M. O., Zoback, M.-L., and Zoback, M.: The World Stress Map database release 2016: Crustal stress pattern across scales, *Tectonophysics*, 744, 484-498, <https://doi.org/10.1016/j.tecto.2018.07.007>, 2018.
- 1382**
- 1383**
- 1384** Holder, J., Olson, J. E., and Philip, Z.: Experimental determination of subcritical crack growth parameters in sedimentary rock, *Geophysical Research Letters*, 28, 599-602, <https://doi.org/10.1029/2000GL011918>, 2001.
- 1385**
- 1386** Hooke, R.: Geomorphic evidence for Late-Wisconsin and Holocene tectonic deformation, Death Valley, California, *GSA Bulletin*, 83, 2073-2098, 10.1130/0016-7606(1972)83[2073:Geflah]2.0.Co;2, 1972.
- 1387**
- 1388** Hooker, J. N., Laubach, S. E., and Marrett, R.: A universal power-law scaling exponent for fracture apertures in sandstones, *GSA Bulletin*, 126, 1340-1362, 10.1130/b30945.1, 2014.
- 1389**
- 1390** Hooker, J. N., Gale, J. F. W., Gomez, L. A., Laubach, S. E., Marrett, R., and Reed, R. M.: Aperture-size scaling variations in a low-strain opening-mode fracture set, Cozzette Sandstone, Colorado, *Journal of Structural Geology*, 31, 707-718, <https://doi.org/10.1016/j.jsg.2009.04.001>, 2009.
- 1391**
- 1392**
- 1393** Hooker, J.N., Laubach, S.E., and Marrett, R.: Fracture-aperture size–frequency, spatial distribution, and growth processes in strata-bounded and non-strata-bounded fractures, Cambrian Mesón Group, NW Argentina, *Journal of Structural Geology*, 54, 54-71, doi.org/10.1016/j.jsg.2013.06.011, 2013.
- 1394**
- 1395**

- 1396** Isherwood, D. and Street, A.: Biotite-induced grossification of the Boulder Creek Granodiorite, Boulder County, Colorado, GSA Bulletin, 87, 366-370, 10.1130/0016-7606(1976)87<366:Bgotbc>2.0.Co;2, 1976.
- 1397**
- 1398** Janio de Castro Lima, J. and Paraguassú, A. B.: Linear thermal expansion of granitic rocks: influence of apparent porosity, grain size and quartz content, Bulletin of Engineering Geology and the Environment, 63, 215-220, 10.1007/s10064-004-0233-x, 2004.
- 1399**
- 1400** Jenny, H.: Factors of Soil Formation: A System of Quantitative Pedology, McGraw-Hill, New York, New York, 1941.
- 1401** Kobayashi, A. S. and Enetanya, A. N.: Stress intensity factor of a corner crack, Mechanics of Crack Growth, 1976.
- 1402** Kranz, R. L.: Microcrack in rocks: A review, Tectonophysics, 100, 449-480, 1983.
- 1403** Krumbein, W. C.: Fundamental attributes of sedimentary particles, University of Iowa Student Engineering Bulletin, 27, 318-331, 1943.
- 1404**
- 1405** Krumbein, W. C. and Sloss, L. L.: Stratigraphy and Sedimentation, W. H. Freeman and Company, San Francisco, California, 1951.
- 1406** Lamp, J. L., Marchant, D. R., Mackay, S. L., and Head, J. W.: Thermal stress weathering and the spalling of Antarctic rocks, Journal of Geophysical Research: Earth Surface, 122, 3-24, <https://doi.org/10.1002/2016JF003992>, 2017.
- 1407**
- 1408** Laubach, S. E., Olson, J. E., and Gross, M. R.: Mechanical and fracture stratigraphy, AAPG Bulletin, 93, 1413-1426, 10.1306/07270909094, 2009.
- 1409**
- 1410** Laubach, S. E., Lamarche, J., Gauthier, B. D. M., Dunne, W. M., and Sanderson, D. J.: Spatial arrangement of faults and opening-mode fractures, Journal of Structural Geology, 108, 2-15, <https://doi.org/10.1016/j.jsg.2017.08.008>, 2018.
- 1411**
- 1412** Laubach, S. E., Lander, R. H., Criscenti, L. J., Anovitz, L. M., Urai, J. L., Pollyea, R. M., Hooker, J. N., Narr, W., Evans, M. A., Kerisit, S. N., Olson, J. E., Dewers, T., Fisher, D., Bodnar, R., Evans, B., Dove, P., Bonnell, L. M., Marder, M. P., and Pyrak-Nolte, L.: The role of chemistry in fracture pattern development and opportunities to advance interpretations of geological materials, Reviews of Geophysics, 57, 1065-1111, 10.1029/2019RG000671, 2019.
- 1413**
- 1414**
- 1415**
- 1416** Leith, K., Moore, J. R., Amann, F., and Loew, S.: In situ stress control on microcrack generation and macroscopic extensional fracture in exhuming bedrock, Journal of Geophysical Research, 119, 1-22, 2014.
- 1417**
- 1418** Leone, J. D., Holbrook, W. S., Reibe, C. S., Chorover, J., Ferre, T. P. A., Carr, B. J., and Callahan, R. P.: Strong slope-aspect control of regolith thickness by bedrock foliation, Earth Surface Processes and Landforms, 45, 2998-3010, 2020.
- 1419**
- 1420** Long, J., Jones, R., Daniels, S., Gilment, S., Oxlade, D., and Wilkinson, M.: Reducing uncertainty in fracture modelling: Assessing user bias in interpretations from satellite imagery, AAPG 2019 Annual Convention & Exhibition, San Antonio, TX, 2019.
- 1421**
- 1422** Long, J. C. S. and Witherspoon, P. A.: The relationship of the degree of interconnection to permeability in fracture networks, Journal of Geophysical Research: Solid Earth, 90, 3087-3098, <https://doi.org/10.1029/JB090iB04p03087>, 1985.
- 1423**
- 1424** Ma, J. et al. Comparison of subcritical crack growth and dynamic fracture propagation in rocks under double-torsion tests. International Journal of Rock Mechanics and Mining Sciences 170, 105481 (2023).
- 1425**
- 1426** Macholdt, D. S., Al-Amri, A. M., Tuffaha, H. T., Jochum, K. P., and Andreae, M. O.: Growth of desert varnish on petroglyphs from Jubbah and Shuwaymis, Ha'il region, Saudi Arabia, The Holocene, 28, 1495-1511, 10.1177/0959683618777075, 2018.
- 1427**
- 1428** Maffucci, R., Bigi, S., Corrado, S., Chiodi, A., Di Paolo, L., Giordano, G., and Invernizzi, C.: Quality assessment of reservoirs by means of outcrop data and "discrete fracture network" models: The case history of Rosario de La Frontera (NW Argentina) geothermal system, Tectonophysics, 647-648, 112-131, <https://doi.org/10.1016/j.tecto.2015.02.016>, 2015.
- 1429**
- 1430**
- 1431** Manzocchi, T.: The connectivity of two-dimensional networks of spatially correlated fractures, Water Resources Research, 38, 1-1-1-20, <https://doi.org/10.1029/2000WR000180>, 2002.
- 1432**
- 1433** Mardia, K. V. and Jupp, P. E.: Directional Statistics, Academic Press Inc., London, England, 1972.
- 1434** Marrett, R., Gale, J. F. W., Gómez, L. A., and Laubach, S. E.: Correlation analysis of fracture arrangement in space, Journal of Structural Geology, 108, 16-33, <https://doi.org/10.1016/j.jsg.2017.06.012>, 2018.
- 1435**
- 1436** Marshall, J., Clyne, J., Eppes, M. C., and Dawson, T.: Barking up the wrong tree? Tree root tapping, subcritical cracking, and potential influence on bedrock porosity, AGU 2021 Fall Abstracts, 2021a.
- 1437**
- 1438** Marshall, J. A., Roering, J. J., Rempel, A. W., Shafer, S. L., and Bartlein, P. J.: Extensive frost weathering across unglaciated North America during the Last Glacial Maximum, Geophysical Research Letters, 48, <https://doi.org/10.1029/2020GL090305>, 2021b.
- 1439**
- 1440**

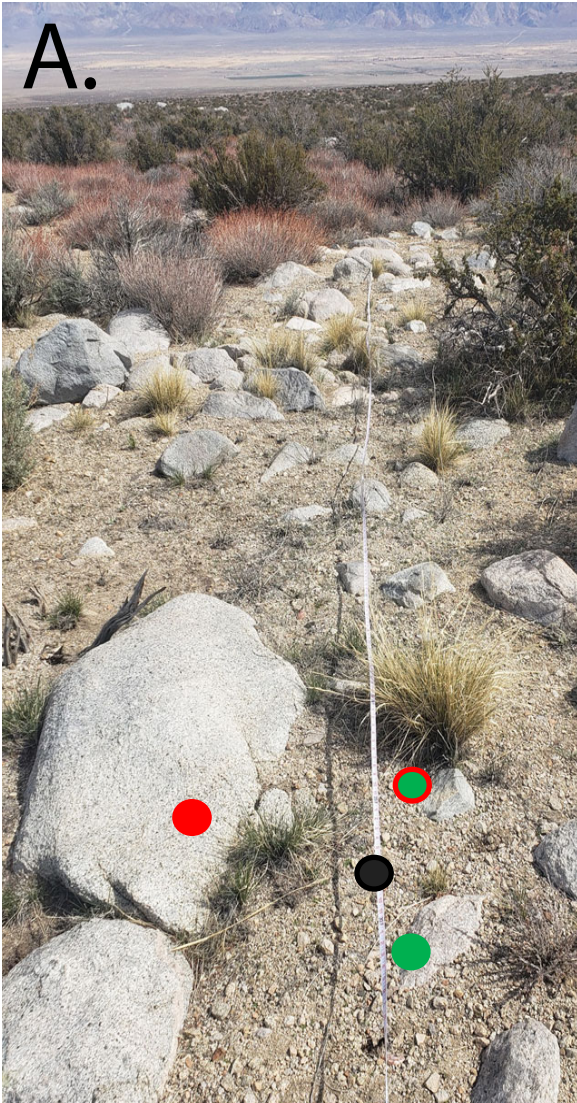
- 1441** Martel, S. J.: Effect of topographic curvature on near-surface stresses and application to sheeting joints, *Geophysical Research Letters*, 33, 2006.
- 1442**
- 1443** Martel, S. J.: Mechanics of curved surfaces, with application to surface-parallel cracks, *Geophysical Research Letters*, 38, 2011.
- 1444** Martel, S. J.: Progress in understanding sheeting joints over the past two centuries, *Journal of Structural Geology*, 94, 68-86, 2017.
- 1445** Matsuoka, N. and Murton, J.: Frost weathering: Recent advances and future directions, *Permafrost and Periglacial Processes*, 19, 195-210, 10.1002/ppp.620, 2008.
- 1446**
- 1447** Matthews, J. A. and Winkler, S.: Schmidt-hammer exposure-age dating: A review of principles and practice, *Earth-Science Reviews*, 230, 104038, <https://doi.org/10.1016/j.earscirev.2022.104038>, 2022.
- 1448**
- 1449** McAuliffe, J. R., McFadden, L. D., Persico, L. P., and Rittenour, T. M.: Climate and vegetation change, hillslope soil erosion, and the complex nature of Late Quaternary environmental transitions, Eastern Mojave Desert, USA, *Quaternary*, 5, 43, 2022.
- 1450**
- 1451** McCarroll, D.: The Schmidt hammer, weathering, and rock surface roughness, *Earth Surface Processes and Landforms*, 16, 477-480, <https://doi.org/10.1002/esp.3290160510>, 1991.
- 1452**
- 1453** McFadden, L. D. and Hendricks, D. M.: Changes in the content and composition of pedogenic iron oxyhydroxides in a chronosequence of soils in southern California, *Quaternary Research*, 23, 189-204, [https://doi.org/10.1016/0033-5894\(85\)90028-6](https://doi.org/10.1016/0033-5894(85)90028-6), 1985.
- 1454**
- 1455**
- 1456** McFadden, L. D., Eppes, M. C., Gillespie, A. R., and Hallet, B.: Physical weathering in arid landscapes due to diurnal variation in the direction of solar heating, *GSA Bulletin*, 117, 161-173, 2005.
- 1457**
- 1458** Mogi, K.: Effect of the intermediate principal stress on rock failure, *Journal of Geophysical Research (1896-1977)*, 72, 5117-5131, <https://doi.org/10.1029/JZ072i020p05117>, 1967.
- 1459**
- 1460** Mogi, K.: Fracture and flow of rocks under high triaxial compression, *Journal of Geophysical Research (1896-1977)*, 76, 1255-1269, <https://doi.org/10.1029/JB076i005p01255>, 1971.
- 1461**
- 1462** Molaro, J. L., Byrne, S., and Le, J.-L.: Thermally induced stresses in boulders on airless body surfaces, and implications for rock breakdown, *Icarus*, 294, 247-261, 2017.
- 1463**
- 1464** Molaro, J. L., Hergenrother, C. W., Chesley, S. R., Walsh, K. J., Hanna, R. D., Haberle, C. W., Schwartz, S. R., Ballouz, R.-L., Bottke, W. F., Campins, H. J., and Lauretta, D. S.: Thermal fatigue as a driving mechanism for activity on asteroid Bennu, *Journal of Geophysical Research*, 125, 1-24, 10.1029/2019JE006325, 2020.
- 1465**
- 1466**
- 1467** Molnar, P.: Interactions among topographically induced elastic stress, static fatigue, and valley incision, *Journal of Geophysical Research*, 109, 1-9, 10.1029/2003JF000097, 2004.
- 1468**
- 1469** Moon, S., Perron, J. T., Martel, S. J., Goodfellow, B. W., Ivars, D. M., Hall, A., Heyman, J., Munier, R., Naslund, J., Simeonov, A., and Stroeven, A. P.: Present-day stress field influences bedrock fracture openness deep into the subsurface, *Geophysical Research Letters*, 47, 1-10, 2020.
- 1470**
- 1471**
- 1472** Moon, S., Perron, J. T., Martel, S. J., Goodfellow, B. W., Mas Ivars, D., Simeonov, A., Munier, R., Naslund, J.-O., Hall, A., Stroeven, A. P., Ebert, K., and Heyman, J.: Landscape features influence bedrock fracture openness in the deep subsurface, *Geological Society of American Annual Meeting*, Phoenix, AZ, USA, 10.1130/abs/2019AM-336309,
- 1473**
- 1474**
- 1475** Moser, F.: Spatial and temporal variance in rock dome exfoliation and weathering near Twain Harte, California, USA, *Geography and Earth Sciences*, The University of North Carolina Charlotte, ProQuest, 2017.
- 1476**
- 1477** Mushkin, A., Sagy, A., Trabelci, E., Amit, R., and Porat, N.: Measure the time and scale-dependency of subaerial rock weathering rates over geologic time scales with ground-based lidar, *Geology*, 42, 1063-1066, 2014.
- 1478**
- 1479** Nara, Y. and Kaneko, K.: Sub-critical crack growth in anisotropic rock, *International Journal of Rock Mechanics and Mining Sciences*, 43, 437-453, <https://doi.org/10.1016/j.ijrmms.2005.07.008>, 2006.
- 1480**
- 1481** Nara, Y., Kashiwaya, K., Nishida, Y., and Ii, T.: Influence of surrounding environment on subcritical crack growth in marble, *Tectonophysics*, 706-707, 116-128, 2017.
- 1482**
- 1483** Nara, Y., Morimoto, K., Hiroyoshi, N., Yoneda, T., Kaneko, K., and Benson, P. M.: Influence of relative humidity on fracture toughness of rock: Implications for subcritical crack growth, *International Journal of Solids and Structures*, 49, 2471-2481, <https://doi.org/10.1016/j.ijsolstr.2012.05.009>, 2012.
- 1484**
- 1485**

- 1486** Narr, W. and Lerche, I.: A method for estimating subsurface fracture density in core, *AAPG Bulletin*, 68, 637-648,
1487 10.1306/ad461354-16f7-11d7-8645000102c1865d, 1984.
- 1488** Neely, A. B., DiBiase, R. A., Corbett, L. B., Bierman, P. R., and Caffee, M. W.: Bedrock fracture density controls on hillslope
1489 erodibility in steep, rocky landscapes with patchy soil cover, southern California, USA, *Earth and Planetary Science Letters*, 522,
1490 186-197, <https://doi.org/10.1016/j.epsl.2019.06.011>, 2019.
- 1491** Ollier, C. D.: *Weathering*, 2nd, Longman, London, England, 1984.
- 1492** Olsen, T., Borella, J., and Stahl, T.: Clast transport history influences Schmidt hammer rebound values, *Earth Surface Processes*
1493 *and Landforms*, 45, 1392-1400, <https://doi.org/10.1002/esp.4809>, 2020.
- 1494** Olson, J. E.: Predicting fracture swarms - the influence of subcritical crack growth and the crack-tip process zone on joint spacing
1495 in rock, *Geological Society of London Special Publications*, 231, 73-87, 2004.
- 1496** Ortega, O. and Marrett, R.: Prediction of macrofracture properties using microfracture information, Mesaverde Group sandstones,
1497 San Juan basin, New Mexico, *Journal of Structural Geology*, 22, 571-588, [https://doi.org/10.1016/S0191-8141\(99\)00186-8](https://doi.org/10.1016/S0191-8141(99)00186-8), 2000.
- 1498** Ortega, O. J., Marrett, R. A., and Laubach, S. E.: A scale-independent approach to fracture intensity and average spacing
1499 measurement, *AAPG Bulletin*, 90, 193-208, 10.1306/08250505059, 2006.
- 1500** Paris, P. and Erdogan, F.: A critical analysis of crack propagation laws, *Journal of Basic Engineering*, 85, 528-533,
1501 10.1115/1.3656900, 1963.
- 1502** Phillips, J. D.: An evaluation of the factors determining the effectiveness of water quality buffer zones, *Journal of Hydrology*, 107,
1503 133-145, [https://doi.org/10.1016/0022-1694\(89\)90054-1](https://doi.org/10.1016/0022-1694(89)90054-1), 1989.
- 1504** Ponti, S., Pezza, M., and Guglielmin, M.: The development of Antarctic tafoni: Relations between differential weathering rates
1505 and spatial distribution of thermal events, salts concentration, and mineralogy, *Geomorphology*, 373, 2021.
- 1506** Ramcharan, A., Hengl, T., Nauman, T., Brungard, C., Waltman, S., Wills, S., and Thompson, J.: Soil property and class maps of
1507 the conterminous United States at 100-meter spatial resolution, *Soil Science Society of America Journal*, 82, 186-201,
1508 <https://doi.org/10.2136/sssaj2017.04.0122>, 2018.
- 1509** Ramulu, M., Chakraborty, A. K., and Sitharam, T. G.: Damage assessment of basaltic rock mass due to repeated blasting in a
1510 railway tunnelling project – A case study, *Tunnelling and Underground Space Technology*, 24, 208-221,
1511 <https://doi.org/10.1016/j.tust.2008.08.002>, 2009.
- 1512** Rasmussen, M., Eppes, M. C., and Berberich, S.: Untangling the impacts of climate, lithology, and time on rock cracking rates and
1513 morphology in arid and semi-arid Eastern California, *AGU Fall Meeting*, New Orleans, LA, 2021.
- 1514** Ravaji, B., Ali-Lagoa, V., Delbo, M., and Wilkerson, J. W.: Unraveling the mechanics of thermal stress weathering rate-effects,
1515 size-effects, and scaling laws., *Journal of Geophysical Research*, 121, 3304-3328, 10.1029/2019JE006019, 2019.
- 1516** Riebe, C. S., Callahan, R. P., Granke, S. B.-M., Carr, B. J., Hayes, J. L., Schell, M. S., and Sklar, L. S.: Anisovolumetric weathering
1517 in granitic saprolite controlled by climate and erosion rate, *Geology*, 1-5, 10.1130/G48191.1, 2021.
- 1518** Rossen, W. R., Gu, Y., and Lake, L. W.: Connectivity and permeability in fracture networks obeying power-law statistics, *SPE*
1519 *Permian Basin Oil and Gas Recovery Conference*, 10.2118/59720-ms, 2000.
- 1520** Røyne, A., Jamtveit, B., Mathiesen, J., and Malthe-Sørenssen, A.: Controls on rock weathering rates by reaction-induced
1521 hierarchical fracturing, *Earth and Planetary Science Letters*, 275, 364-369, <https://doi.org/10.1016/j.epsl.2008.08.035>, 2008. Rysak,
1522 B., Gale, J. F., Laubach, S. E., & Ferrill, D. A.: Mechanisms for the generation of complex fracture networks: Observations from
1523 slant core, analog models, and outcrop, *Frontiers in Earth Science*, 10, 848012, 2022.
- 1524** Sanderson, D. J.: Field-based structural studies as analogues to sub-surface reservoirs, *Geological Society, London, Special*
1525 *Publications*, 436, 207-217, doi:10.1144/SP436.5, 2016.
- 1526** Sanderson, D. J. and Nixon, C. W.: Topology, connectivity and percolation in fracture networks, *Journal of Structural Geology*,
1527 115, 167-177, <https://doi.org/10.1016/j.jsg.2018.07.011>, 2018.
- 1528** Scarciglia, F., Saporito, N., La Russa, M. F., Le Pera, E., Macchione, M., Puntillo, D., Crisci, G. M., and Pezzino, A.: Role of
1529 lichens in weathering of granodiorite in the Sila uplands (Calabria, Southern Italy), *Sedimentary Geology*, 280, 119-134, 2012.
- 1530** Schoeneberger, P. J., Wysocki, D. A., and Benham, E. C.: *Field Book for Describing and Sampling Soils: Version 3.0*, Natural
1531 Resources Conservation Service, National Soil Survey Center, Lincoln, Nebraska 2012.

- 1532** Schultz, R. A.: *Geologic Fracture Mechanics*, Cambridge University Press, Cambridge, England, DOI: 10.1017/9781316996737, 2019.
1533
- 1534** Shakiba, M., Lake, L.W., Gale, J.F.W., Laubach, S.E., Pyrcz, M.J.: Multiscale spatial analysis of fracture nodes in two dimensions, *Marine & Petroleum Geology*, 149, 106093, doi.org/10.1016/j.marpetgeo.2022.106093, 2023.
1535
- 1536** Sharifigaliuk, H., Mahmood, S. M., Ahmad, M., and Rezaee, R.: Use of outcrop as substitute for subsurface shale: Current understanding of similarities, discrepancies, and associated challenges, *Energy & Fuels*, 35, 9151-9164, 10.1021/acs.energyfuels.1c00598, 2021.
1537
1538
- 1539** Shi, J.: *Study of thermal stresses in rocks due to diurnal solar exposure*, Civil Engineering, University of Washington, 58 pp., 2011.
- 1540** Shobe, C. M., Hancock, G. S., Eppes, M. C., and Small, E. E.: Field evidence for the influence of weathering on rock erodibility and channel form in bedrock rivers, *Earth Surface Processes and Landforms*, 42, 1997-2012, 2017.
1541
- 1542** Sklar, L. S., Riebe, C. S., Marshall, J. A., Genetti, J., Leclere, S., Lukens, C. L., and Merces, V.: The problem of predicting the size distribution of sediment supplied by hillslopes to rivers, *Geomorphology*, 277, 31-49, 2017.
1543
- 1544** Snowdon, A. P., Normani, S. D., and Sykes, J. F.: Analysis of crystalline rock permeability versus depth in a Canadian Precambrian rock setting, *Journal of Geophysical Research: Solid Earth*, 126, e2020JB020998, https://doi.org/10.1029/2020JB020998, 2021.
1545
- 1546** Sousa, L. M. O.: Evaluation of joints in granitic outcrops for dimension stone exploitation, *Quarterly Journal of Engineering Geology and Hydrogeology*, 43, 85-94, 10.1144/1470-9236/08-076, 2010.
1547
- 1548** St. Clair, J., Moon, S., Holbrook, W. S., Perron, J. T., Riebe, C. S., Martel, S. J., Carr, B., Harman, C., Singha, K., and Richter, D. D.: Geophysical imaging reveals topographic stress control of bedrock weathering, *Geomorphology*, 350, 534-538, 2015.
1549
- 1550** Staff, Soil Survey: *Soil Taxonomy: A basic system of soil classification for making and interpreting soil surveys*, 1999.
- 1551** R.D. Terzaghi: Sources of error in joint surveys, *Geotechnique*, 15, 287-304, 1965.
- 1552** Terry, R. D. and Chilingar, G. V.: Summary of "Concerning some additional aids in studying sedimentary formations," by M. S. Shvetsov, *Journal of Sedimentary Research*, 25, 229-234, 10.1306/74d70466-2b21-11d7-8648000102c1865d, 1955.
1553
- 1554** Turner, F. J., Griggs, D. T., and Heard, H. C.: Experimental deformation of calcite crystals, *GSA Bulletin*, 65, 883-934, 10.1130/0016-7606(1954)65[883:Edocc]2.0.Co;2, 1954.
1555
- 1556** Ukar, E., Laubach, S. E., and Hooker, J. N.: Outcrops as guides to subsurface natural fractures: Example from the Nikanassin Formation tight-gas sandstone, Grande Cache, Alberta foothills, Canada, *Marine and Petroleum Geology*, 103, 255-275, https://doi.org/10.1016/j.marpetgeo.2019.01.039, 2019.
1557
1558
- 1559** Ulusay, R. and Hudson, J. A.: *The Complete ISRM Suggested Methods for Rock Characterization, Testing and Monitoring: 1974-2006*, Commission on Testing Methods, International Society of Rock Mechanics., Ankara, Turkey 2007.
1560
- 1561** Ulusay, R. (ed.), 2015. *The ISRM suggested methods for rock characterization, testing and monitoring: 2007–2014*. Springer, Cham, Switzerland. DOI:10.1007/978-3-319-007713-0."Vazquez, P., Shushakova, V., and Gomez-Heras, M.: Influence of mineralogy on granite decay induced by temperature increase: Experimental observations and stress simulation, *Engineering Geology*, 189, 58-67, 2015.
1562
1563
1564
- 1565** Viswanathan, H.S., et al: From fluid flow to coupled processes in fractured rock: recent advances and new frontiers, *Reviews of Geophysics*, 60(1), e2021RG000744, 2022.
1566
- 1567** Wang, H. F., Bonner, B. P., Carlson, S. R., Kowallis, B. J., and Heard, H. C.: Thermal stress cracking in granite, *Journal of Geophysical Research: Solid Earth*, 94, 1745-1758, https://doi.org/10.1029/JB094iB02p01745, 1989.
1568
- 1569** Wang, Q., Narr, W., Laubach, S.E.: Quantitative characterization of fracture spatial arrangement and intensity in a reservoir anticline using horizontal wellbore image logs and an outcrop analog, *Marine & Petroleum Geology*, 152, 106238, https://doi.org/10.1016/j.marpetgeo.2023.106238, 2023.
1570
1571
- 1572** Watkins, H., Bond, C. E., Healy, D., and Butler, R. W. H.: Appraisal of fracture sampling methods and a new workflow to characterise heterogeneous fracture networks at outcrop, *Journal of Structural Geology*, 72, 67-82, https://doi.org/10.1016/j.jsg.2015.02.001, 2015.
1573
1574
- 1575** Weiserbs, B. I.: *The morphology and history of exfoliation on rock domes in the Southeastern United States*, Geography and Earth Sciences, The University of North Carolina Charlotte, ProQuest, 2017.
1576

- 1577** Weiss, M.: Techniques for estimating fracture size: A comparison of methods, *International Journal of Rock Mechanics and Mining Sciences*, 45, 460-466, <https://doi.org/10.1016/j.ijrmms.2007.07.010>, 2008.
- 1578**
- 1579** Wenk, H.-R.: Some roots of experimental rock deformation, *Bulletin de Mineralogie*, 102, 195-202, <https://doi.org/10.3406/bulmi.1979.7277>, 1979.
- 1580**
- 1581** West, N., Kirby, E., Bierman, P. R., and Clarke, B. A.: Aspect-dependent variations in regolith creep revealed by meteoric ¹⁰Be, *Geology*, 42, 507-510, 10.1130/g35357.1, 2014.
- 1582**
- 1583** Whitmeyer, S., Pyle, E., Pavlis, T., Swanger, W. & Roberts, L.: Modern approaches to field data collection and mapping: Digital methods, crowdsourcing, and the future of statistical analyses, *Journal of Structural Geology*, 125, 29-40, 2019.
- 1584**
- 1585** Wohl, E. E.: The effect of bedrock jointing on the formation of straths in the Cache la Poudre River drainage, Colorado Front Range, *Journal of Geophysical Research: Earth Surface*, 113, <https://doi.org/10.1029/2007JF000817>, 2008.
- 1586**
- 1587** Wolman, M. G.: A method of sampling coarse river-bed material, *Eos, Transactions American Geophysical Union*, 35, 951-956, <https://doi.org/10.1029/TR035i006p00951>, 1954.
- 1588**
- 1589** Wu, H. and Pollard, D. D.: An experimental study of the relationship between joint spacing and layer thickness, *Journal of Structural Geology*, 17, 887-905, [https://doi.org/10.1016/0191-8141\(94\)00099-L](https://doi.org/10.1016/0191-8141(94)00099-L), 1995.
- 1590**
- 1591** Zeeb, C., Gomez-Rivas, E., Bons, P. D., and Blum, P.: Evaluation of sampling methods for fracture network characterization using outcrops, *AAPG Bulletin*, 97, 1545-1566, 10.1306/02131312042, 2013.
- 1592**
- 1593** Zeng, Fan, Biao Shu, and Qiwu Shen. "A combination of Light Detection and Ranging with Digital Panoramic Borehole Camera System in fracture mapping to characterize discrete fracture networks." *Bulletin of Engineering Geology and the Environment* 82, no. 7, 249, <https://doi.org/10.1007/s10064-023-03274-5> , 2023:
- 1594**
- 1595**
- 1596** Zhang, C., Hu, X., Wu, Z., and Li, Q.: Influence of grain size on granite strength and toughness with reliability specified by normal distribution, *Theoretical and Applied Fracture Mechanics*, 96, 534-544, <https://doi.org/10.1016/j.tafmec.2018.07.001>, 2018.
- 1597**
- 1598** Zhang, L.: Determination and applications of rock quality designation (RQD), *Journal of Rock Mechanics and Geotechnical Engineering*, 8, 389-397, <https://doi.org/10.1016/j.jrmge.2015.11.008>, 2016.
- 1599**
- 1600** Zhou, W., Shi, G., Wang, J., Liu, J., Xu, N., and Liu, P.: The influence of bedding planes on tensile fracture propagation in shale and tight sandstone, *Rock Mechanics and Rock Engineering*, 55, 1111-1124, 10.1007/s00603-021-02742-2, 2022.
- 1601**
- 1602**

FIGURE 1



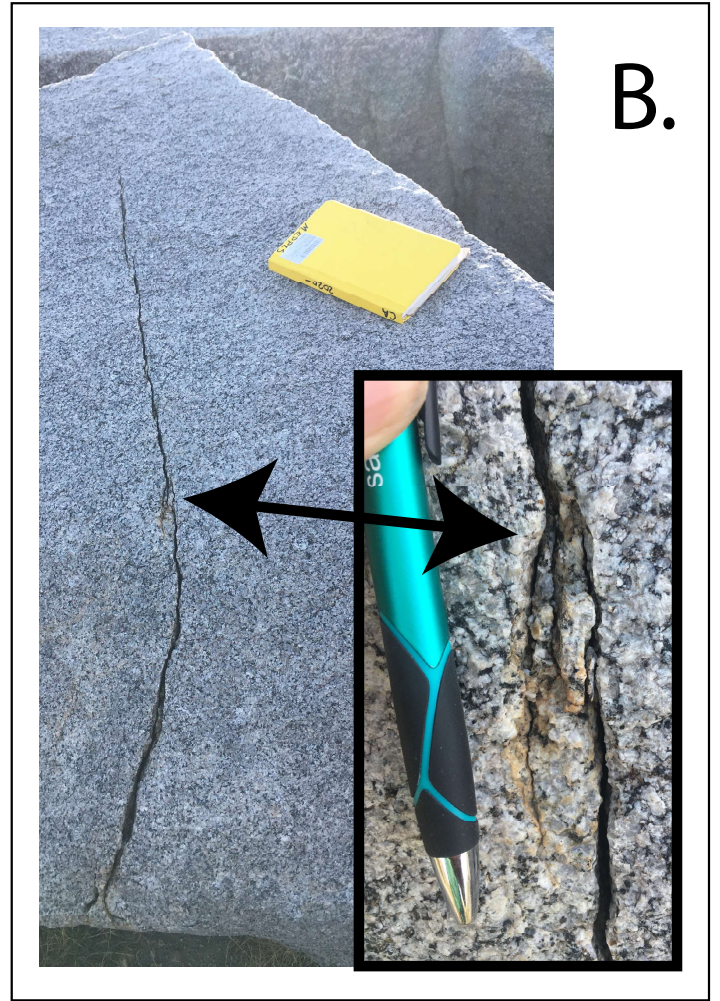
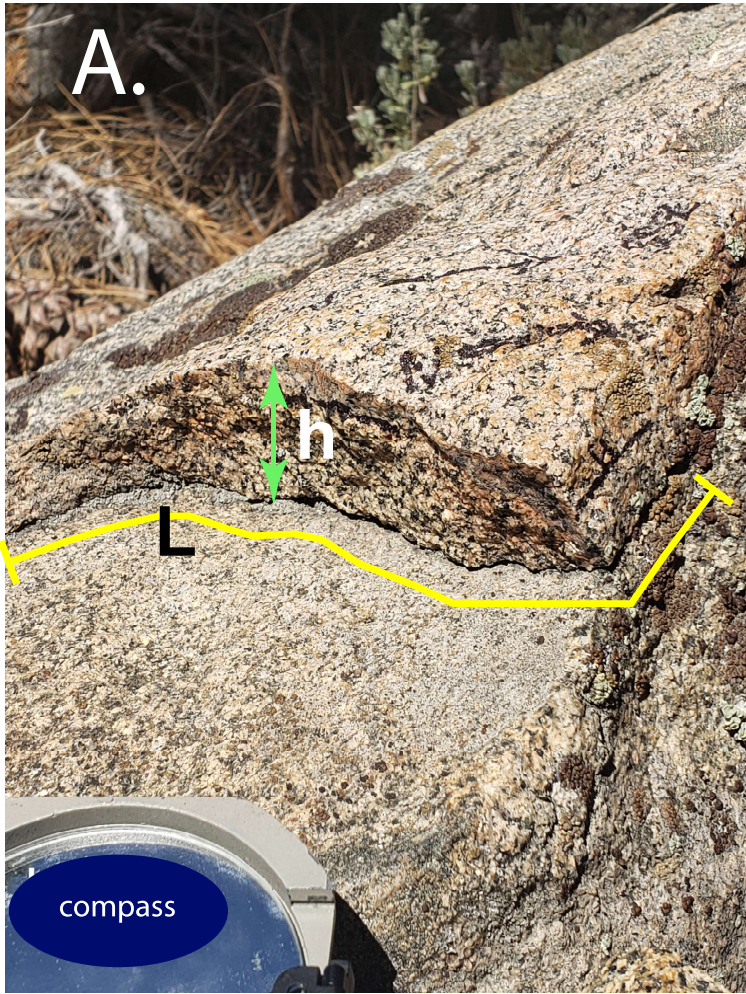


FIGURE 3

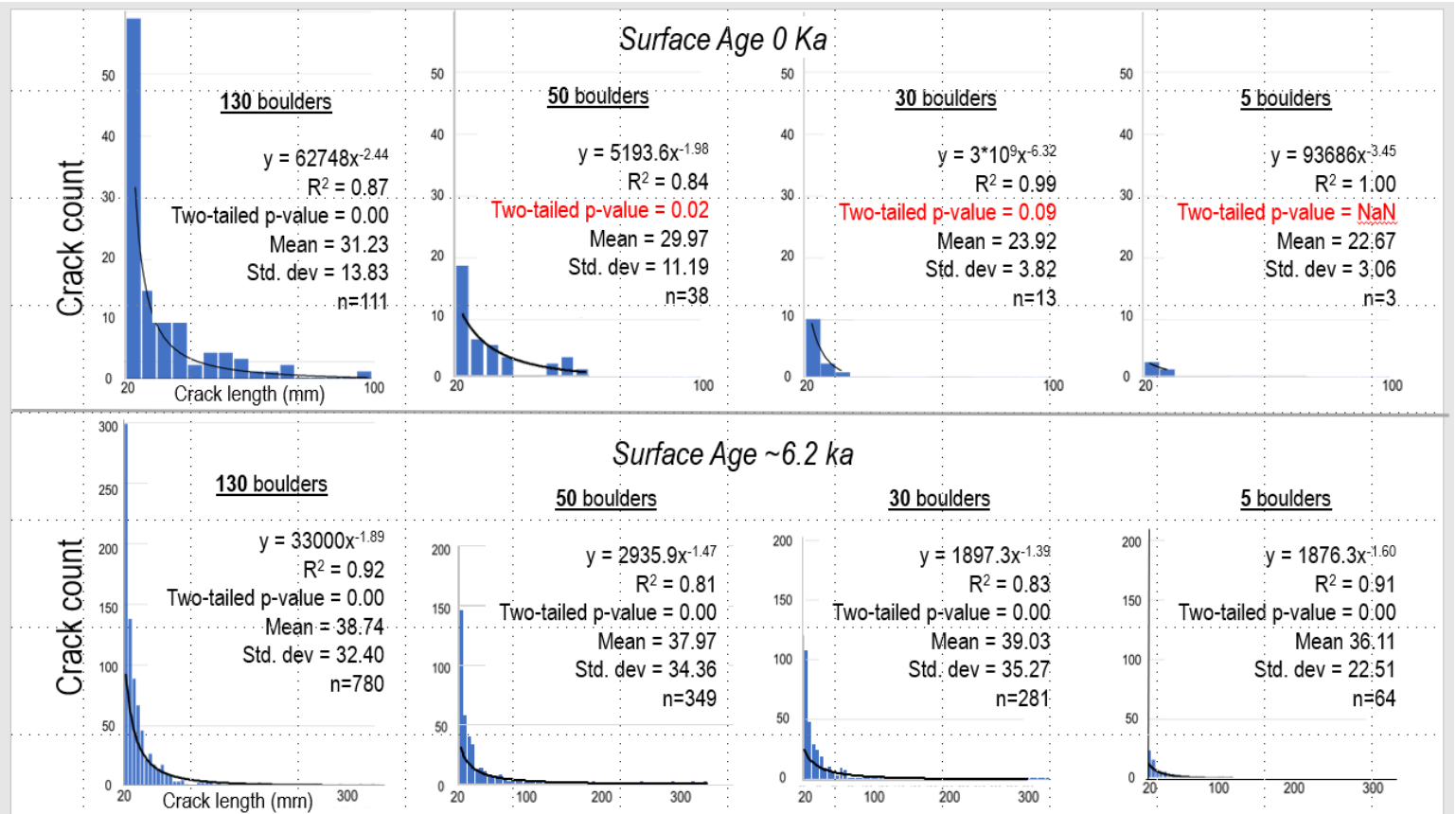


Fig. 3

FIGURE 4

Name(s) & Date:		Criteria for Clast/Outcrop selection:										Relevant Cl, O, R, P, T observations:				
Site Name:												Vegetation-type & percent of each:				
GPS Coordinates:												open ground cover (%):				
GPS Projection:		Portion observed (eg. All exposed, north face only, etc.):										Surface Slope:				
Orientation conventions:												Other:				
Declination:																

ID & Rock Type	Avg. Grain Size (mm)	spheri- city/ round- ness	Mineralogy	Length (cm)	Width (cm)	Height (cm)	Exposure	Cracks cm	GD & Pit	Lichen	Varnish	Fabric Type	Fabric Strike (°)	Fabric Dip (°)	Crack ID	Crack Parallel to	Mid Crack Width (mm)	Crack Max Width (mm)	Crack Length (mm)	Crack Strike (°)	Crack Dip (°)	Sheet Ht. (mm)	Weathering Index	Notes		
s- r-							0123	012345	gp	012345	012345	FSBVO				SFL								1 2 3 4 5		
s- r-							0123	012345	gp	012345	012345	FSBVO				SFL									1 2 3 4 5	
s- r-							0123	012345	gp	012345	012345	FSBVO				SFL									1 2 3 4 5	
s- r-							0123	012345	gp	012345	012345	FSBVO				SFL									1 2 3 4 5	
s- r-							0123	012345	gp	012345	012345	FSBVO				SFL									1 2 3 4 5	
s- r-							0123	012345	gp	012345	012345	FSBVO				SFL									1 2 3 4 5	
s- r-							0123	012345	gp	012345	012345	FSBVO				SFL									1 2 3 4 5	
s- r-							0123	012345	gp	012345	012345	FSBVO				SFL									1 2 3 4 5	
s- r-							0123	012345	gp	012345	012345	FSBVO				SFL									1 2 3 4 5	
s- r-							0123	012345	gp	012345	012345	FSBVO				SFL									1 2 3 4 5	
s- r-							0123	012345	gp	012345	012345	FSBVO				SFL									1 2 3 4 5	
s- r-							0123	012345	gp	012345	012345	FSBVO				SFL									1 2 3 4 5	
s- r-							0123	012345	gp	012345	012345	FSBVO				SFL									1 2 3 4 5	
s- r-							0123	012345	gp	012345	012345	FSBVO				SFL									1 2 3 4 5	
s- r-							0123	012345	gp	012345	012345	FSBVO				SFL									1 2 3 4 5	
s- r-							0123	012345	gp	012345	012345	FSBVO				SFL									1 2 3 4 5	
s- r-							0123	012345	gp	012345	012345	FSBVO				SFL									1 2 3 4 5	
s- r-							0123	012345	gp	012345	012345	FSBVO				SFL									1 2 3 4 5	
s- r-							0123	012345	gp	012345	012345	FSBVO				SFL									1 2 3 4 5	
s- r-							0123	012345	gp	012345	012345	FSBVO				SFL									1 2 3 4 5	
s- r-							0123	012345	gp	012345	012345	FSBVO				SFL									1 2 3 4 5	
s- r-							0123	012345	gp	012345	012345	FSBVO				SFL									1 2 3 4 5	
s- r-							0123	012345	gp	012345	012345	FSBVO				SFL									1 2 3 4 5	
s- r-							0123	012345	gp	012345	012345	FSBVO				SFL									1 2 3 4 5	
s- r-							0123	012345	gp	012345	012345	FSBVO				SFL									1 2 3 4 5	
s- r-							0123	012345	gp	012345	012345	FSBVO				SFL									1 2 3 4 5	
s- r-							0123	012345	gp	012345	012345	FSBVO				SFL									1 2 3 4 5	

<p>Cracks <2 cm: Evidence of microcracks <2 cm long, 0 = 0; 1 = <1/dm²; 2 = 1-5/dm²; 3 = 5-10/dm²; 4 = >10/dm²</p> <p>GD & Pit: G = positive evidence of granular disintegration (loose grains) P = pitting evident</p> <p>Crack length defined as total exposed length of the crack; equivalent to a surface exposure length NOT a 'caliper' length.</p> <p>Fabric type: f=foliation; s=fossils; b=bedding; v = vein or dyke o=other</p> <p>Lichen & varnish: 0 = 0%, 1 => 0 and <10; 2 => 10 and <30; 3 => 30 and <60; 4 = >60 and <90; 5 => 90</p> <p>Avg. Grain Size = representative size of grains throughout the boulder</p> <p>Parallel: S = surface, F = fabric, L = long axis of clast or outcrop</p> <p>Sheet Ht = the height of the spall or exfoliation resulting from a surface-parallel crack; n/a for other cracks</p>	<p>Crack Parallel to: S: Surface, F: Fabric (joints, bedding); L = long axis</p> <p>weathering Index:</p> <p>0 = no crack (step)</p> <p>1: fresh with evidence of recent rupture (flakes/pieces)</p> <p>2: sharp, no rounded edges anywhere</p> <p>3: mostly sharp with occasional rounded edges</p> <p>4: mostly rounded edges with occasional sharp</p> <p>5: all rounded edges</p> <p>NOTE: 0, or 1 must have clear evidence of a recent break: i.e. small pieces left</p>	<p>Exposure</p> <p>use angle of the boulder at the ground</p> <p>0 1 -2 3</p>
---	--	--

FIGURE 5

Feature (crack, fossil, pore)
Size Classes (mm)

VC = Very Coarse (>20)
C = Coarse (<10 and >5)
M = Medium (<5 and >2)
F = Fine (<2 and >1)
VF = Very Fine (<1)

Quantity Classes

'1' - Few: < 1 per area
 '2' - Common: 1-5 per area
 '3' - Very common: > 5 and < 10 per area
 '4' - Many: ≥ 10 per area

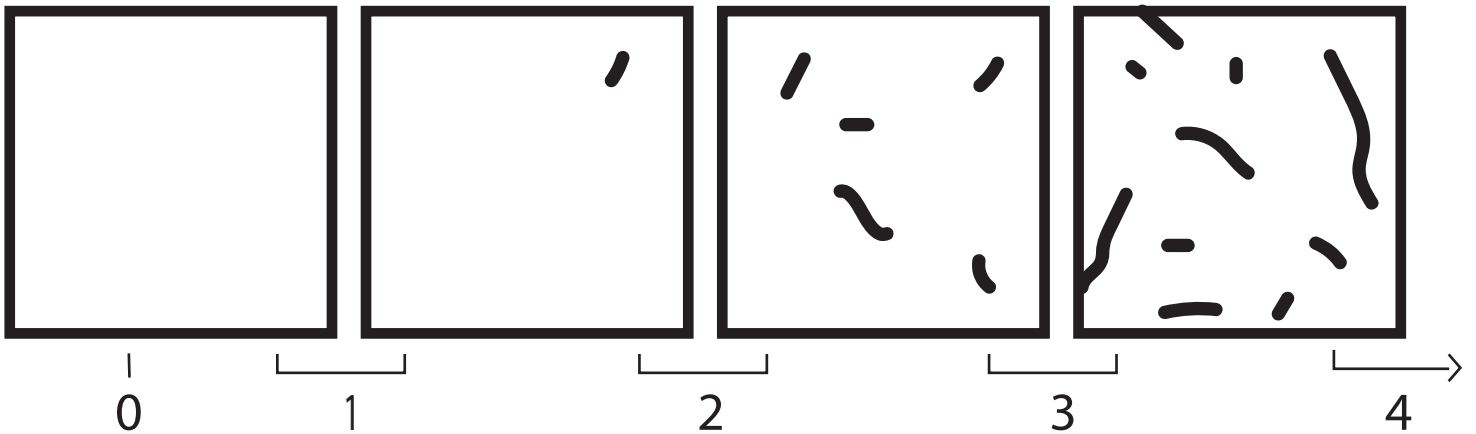
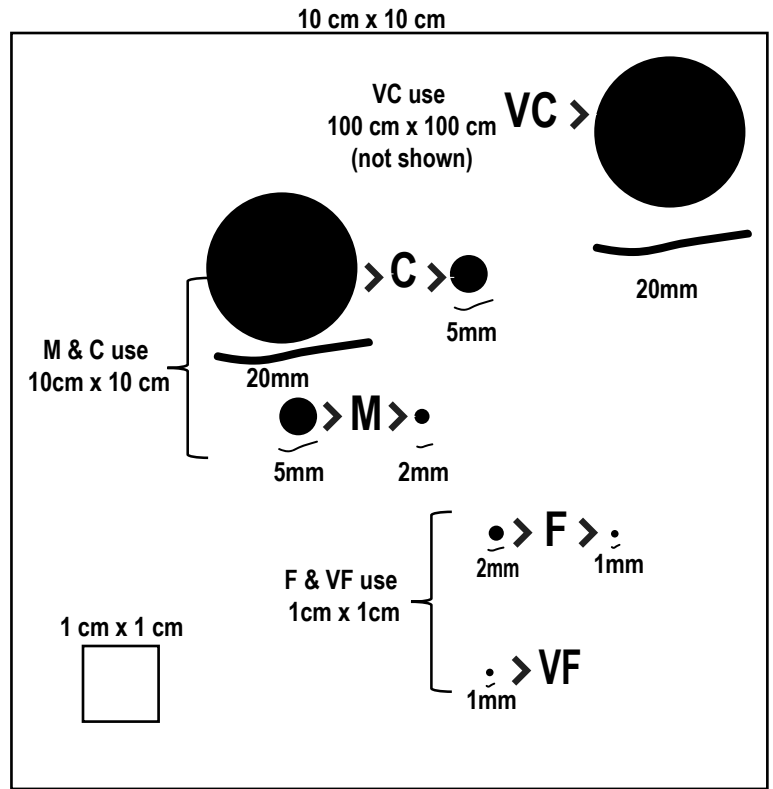


FIGURE 6

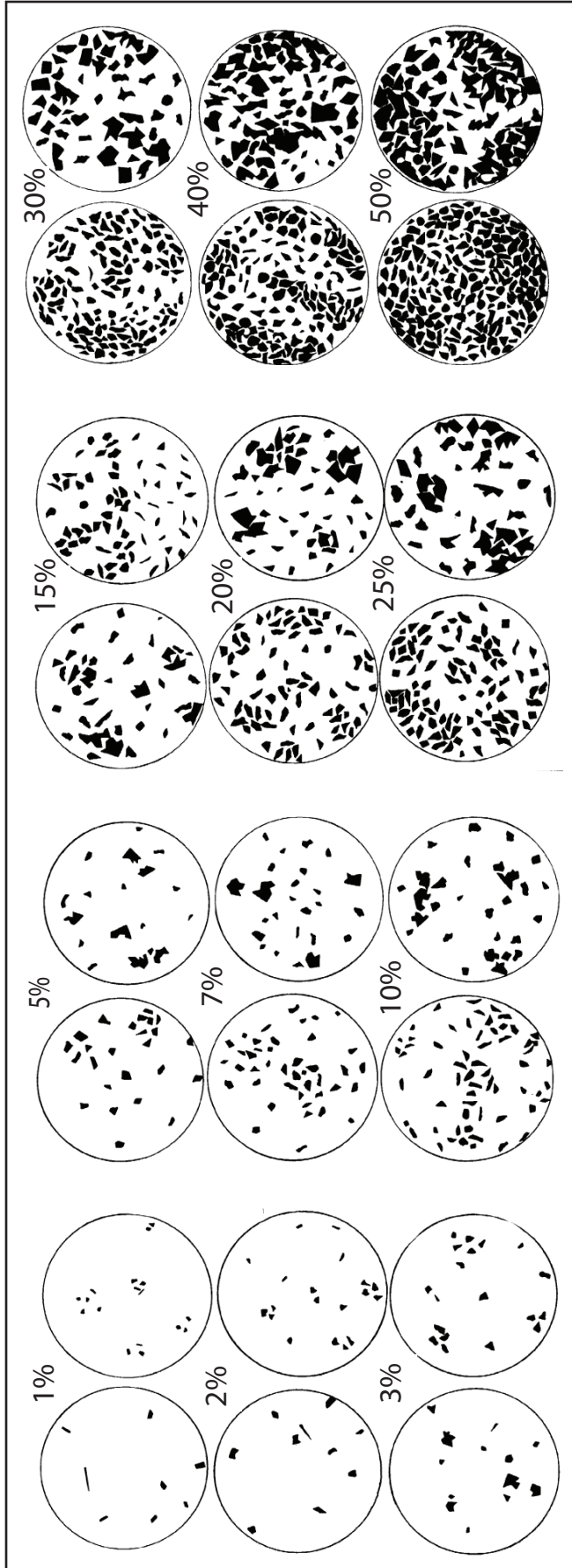
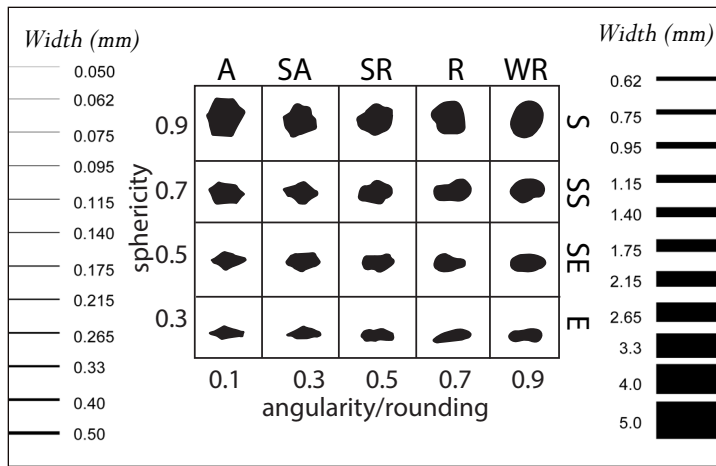


FIGURE 7



note to copy-editor: this figure should be published to scale when the document is viewed at 100%

FIGURE 8

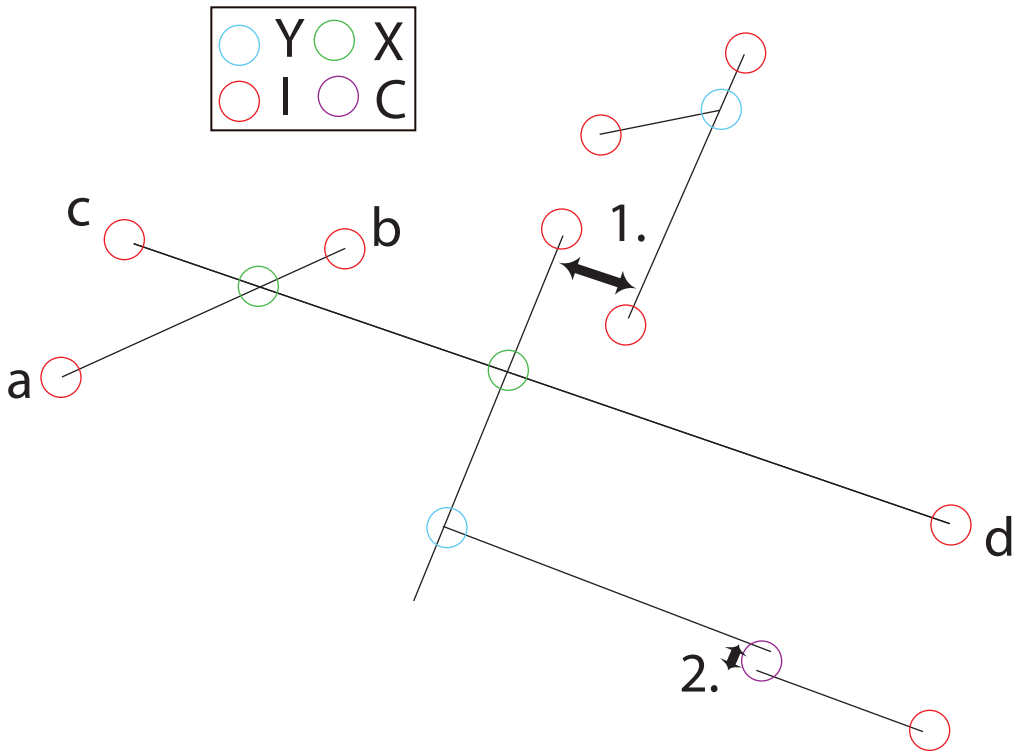


FIGURE 9

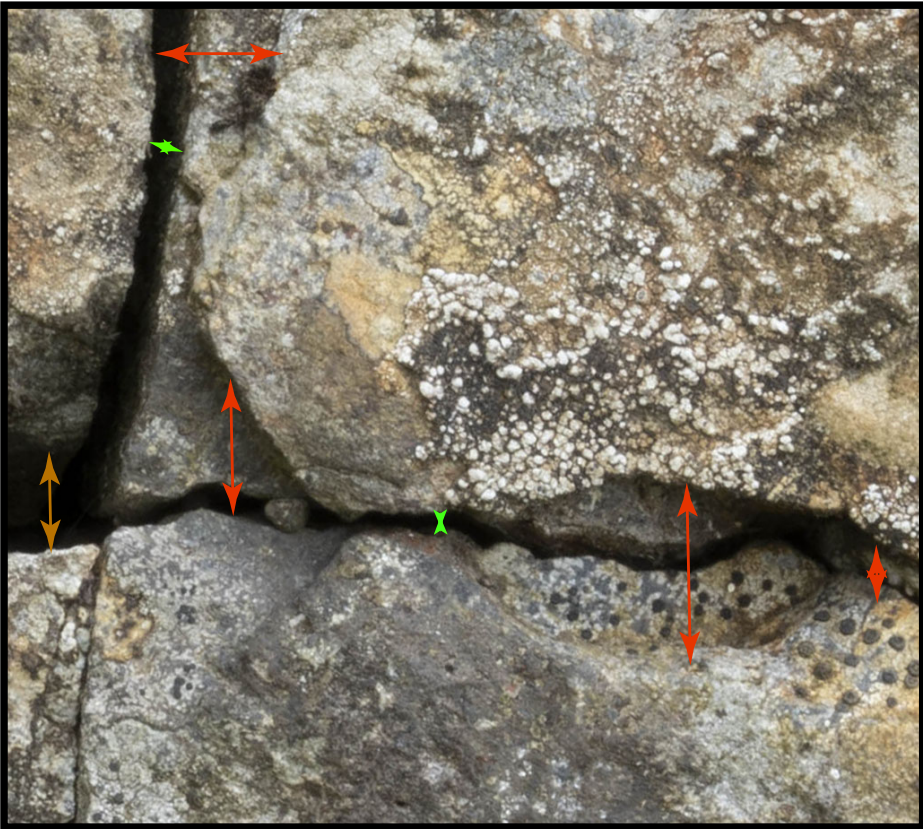


FIGURE 10

